Fig. 2

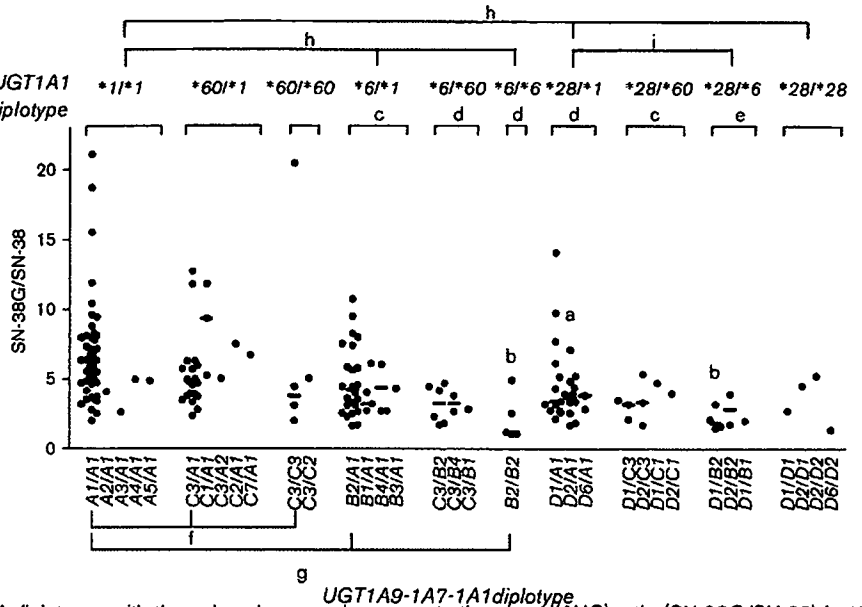

The association of *UGT1A* diplotypes with the reduced area under concentration curve (AUC) ratio (SN-38G/SN-38) in 176 Japanese cancer patients who received irinotecan. The whole gene (*1A9-1A7-1A1*) diplotypes are shown below the abscissa and the *UGT1A1* diplotypes are indicated in the upper part of the figure. Each point represents a patient value, and the median is indicated by a bar. Significant reductions in the AUC ratio were detected in the *B2/B2*, *D2/A1*, and *D1/B2* compared with *A1/A1* for the whole gene diplotypes [Kruskal–Wallis test ($P=0.0009$) followed by Dunnett's multiple comparison test]. As for the *1A1* diplotypes, significant reductions were detected in the **6/*1*, **6/*60*, **6/*6*, **28/*1*, **28/*60*, and **28/*6* compared with the **1/*1* group [Kruskal–Wallis test ($P<0.0001$) followed by Dunnett's multiple comparison test]. Gene–dose effects on the reduced AUC ratio were significant for **6* and **28* (Jonckheere–Terpestra test). A significant additive effect of **6* on the reduced AUC ratio by **28* was detected by comparing **28/*1* and **28/*6*. [a]$P<0.05$ and [b]$P<0.01$ against *A1/A1* group (Dunnett's multiple comparison test); [c]$P<0.05$, [d]$P<0.01$, and [e]$P<0.001$ against the **1/*1* group (Dunnett's multiple comparison test); [f]$P<0.05$, [g]$P<0.001$, and [h]$P<0.0001$ (Jonckheere–Terpestra test for gene–dose effect); [i]$P<0.01$ (Wilcoxon test).

($P = 0.1134$). No significant effects on the AUC ratio were observed for Block C (exon 2–5) haplotypes or rare variations including *1A10* (**2T*, **2*, or **3*) and *1A9* (**5*, **T11*).

Multiple regression analysis of the area under concentration curve ratio

We further assessed the impact of *UGT1A* genetic factors on the AUC ratio by multiple regression analysis. First, we used the *1A9-1A7-1A1* and Block C haplotypes as genetic factors. The AUC ratio was significantly associated with the haplotypes *B2*, *D1*, and *D2* and serum biochemistry parameters indicating hepatic or renal function before treatment. The Groups B and D haplotypes harbor *1A1*6* and **28*, respectively. The dependency on specific *1A7* or *1A9* polymorphisms, however, was not obtained, considering the contributions of both *D1* and *D2*. As *1A1*6* and **28* are mutually exclusive and their effects are comparable, we grouped *1A1*6* and **28* into the same category in the final multiple regression model (Table 4). The final model confirmed the significant contribution of this genetic marker (**6* or **28*) to the AUC ratio.

Effects of the genetic marker '*6 or *28' on pharmaco kinetic parameters

Then, a dose effect of the genetic marker '**6* or **28*' on pharmacokinetic parameters was further analyzed (Fig. 3). Patients with one haplotype harboring either **6* or **28* (**6/*1*, **6/*60*, **28/*1*, and **28/*60*) had lower SN-38G/SN-38 AUC ratios (median, 3.62; interquartile range, 2.74–5.18) than patients without **6* or **28* (**1/*1*, **60/*1*, and **60/*60*) (5.55, 4.13–7.26), and patients with two haplotypes harboring **6* or **28* (**6/*6*, **28/*28*, and **28/*6*) had the lowest AUC ratio (2.07, 1.45–3.62) ($P < 0.0001$, Fig. 3a). Similarly, the number of the **6* or **28*-containing haplotypes affected the AUC ratios of SN-38 to irinotecan (Fig. 3b). When the correlations

Table 3 AUC ratio of SN-38 glucuronide to SN-38 for *UGT1A1* diplotypes

Diplotype	Number of patients	AUC ratio		*P*-value[a] (vs. **1/*1*)
		Median	Interquartile range	
**1/*1*	55	6.13	4.72–7.79	
**1/*60*	25	5.04	3.85–6.52	0.9803
**60/*60*	5	4.48	2.57–12.74	0.8141
**6/*1*	32	4.03	2.74–5.97	0.0126
**6/*60*	9	2.84	2.09–4.33	0.0021
**6/*6*	5	1.19	1.06–3.74	0.0012
**28/*1*	26	3.65	2.76–5.21	0.0040
**28/*60*	8	3.44	2.68–4.40	0.0261
**28/*6*	7	2.03	1.65–3.26	<0.0001
**28/*28*	4	3.65	2.05–4.92	0.2322

AUC, area under concentration curve.
[a]Dunnett's multiple comparison test.

between irinotecan dosage and the AUC of SN-38 were tested, different correlations were obtained according to the number of the haplotypes (Fig. 3c). The slope of regression line for one and two haplotypes harboring **6* or **28* was 1.4-fold and 2.4-fold greater, respectively, than that for the diplotype without **6* or **28*.

Associations of UGT1A1 genetic polymorphisms with toxicities

Association between genetic polymorphisms and toxicities was investigated in patients receiving irinotecan as a single agent. One patient was referred to another hospital 3 days after the first administration of irinotecan without evaluating toxicities and was lost in terms of follow-up. Therefore, association between genetic polymorphisms and toxicities was investigated in 55 patients. Six (11%) and 14 (25%) patients experienced grade 3 or greater diarrhea and neutropenia, respectively. As for the *1A9-1A7-1A1* diplotypes, a higher incidence of grade 3 or greater neutropenia was observed in *D1/B2* (*1A1*28/*6*) (100%, $n = 3$) than in *A1/A1* (11.8%, $n = 17$) ($P = 0.0088$, Fisher's exact test), indicating clinical impact of the genetic marker *1A1*6* or **28*. As for the dose effect of '**6 or *28*', incidences of grade 3 or 4 neutropenia were 14, 24, and 80% for 0, 1, and 2 haplotypes harboring these markers, respectively (Table 5). A significant association between '**6* or **28*'and neutropenia was also observed for 62 patients who received irinotecan in combination with cisplatin (Table 5). No association, however, was observed between diarrhea and the marker '**6* or **28*'.

Multivariate analysis for irinotecan toxicities

We further evaluated the effect of the genetic marker '**6* or **28*' on neutropenia in multivariate analysis, and confirmed a significant correlation of '**6* or **28*' with the nadir of absolute neutrophil counts (Table 6). Elevated alkaline phosphatase levels and the absolute neutrophil count at baseline were also significant.

Discussion

The association study with the *1A9-1A7-1A1* diplotypes revealed that the reduction in inactivation of SN-38, as well as neutropenia, was dependent on the Groups B and D haplotypes which corresponded to the *1A1*6* and **28* segmental haplotypes. Also, multivariate analyses clearly showed clinical significance of the genetic marker '**6* or **28*' for both pharmacokinetics and toxicity of irinotecan in Japanese patients (Tables 3 and 6). *UGT1A1*6* and **28* were mutually exclusive [14] and contributed to the reduction in glucuronidation of SN-38 to the same extent. Therefore, the activity of SN-38 glucuronidation in individuals depended on the number of the haplotypes harboring **6* or **28*. Although the role of *1A1*28* for irinotecan toxicity has been focused on [8–12], this study strongly suggests that **6* should be tested in addition to **28* before starting chemotherapy with irinotecan in Japanese patients.

The clinical importance of **6* for neutropenia by irinotecan was also supported by a recent report in Korean patients who received irinotecan and cisplatin [31]. Although no patients with irinotecan as a single agent were homozygous for **6* in our study, clinical significance of the double heterozygote, **6/*28*, was clearly demonstrated. Among patients treated with irinotecan in combination chemotherapy, the majority of patients received platinum agents in our study. A significant association of '**6* or **28*' with a higher incidence of grade 3 or 4 neutropenia was also observed in patients who received irinotecan and cisplatin (Table 5). These findings further support the necessity of testing '**6* or **28*' before irinotecan is given to patients.

As possible enhancement of toxicities by the **27* allele was suggested [8], we evaluated the effect of the **28c* haplotype, which had an additional single-nucleotide polymorphism [**27*; 686C > A(P229Q)] to the **28* allele (-40_-39insTA). In our cohort of patients, there were three **28c* heterozygotes (**28c/*1*) and one double heterozygote (**28b/*28c*). The values of the AUC ratio were within the range of variations of the **28* group, and no additional impact of **28c* was observed in relation to toxicities.

Although the decreasing trend of the AUC ratio for *1A1*60* (and combinatorial haplotype *C3*) was observed (Fig. 2), the contribution of *1A1*60* to toxicities was not clearly demonstrated in this study as reported in the Japanese retrospective study [32].

In addition to UGT1A1, recent studies have suggested possible contributions of UGT1A7, 1A9, and 1A10 to SN-38G formation [15–17]. An in-vitro study demonstrated that *1A7*3* [387T > G(N129K), 391C > A(R131K), 622T > C(W208R)] had reduced activity in terms of SN-38G formation [16]. Results of clinical studies, however, on the association between *1A7* polymorphisms and irinotecan toxicity/efficacy are inconsistent, whereas different populations with different combination therapies were used [19,20]. Furthermore, it was reported that the *UGT1A7* polymorphisms (**2* and **3*), which were linked to *1A9*1*, were associated with a lowered incidence

Table 4 Multiple regression analysis toward the AUC ratio (SN-38G/SN-38)[a]

Variable	Coefficient	F-value	P-value	R^2	Intercept	N
				0.410	0.8869	176
**6 or *28*	-0.189	70.2	<0.0001			
Age	0.005	8.88	0.0033			
Serum albumin level[b]	-0.136	9.92	0.0019			
Serum GOT and ALP[c]	0.070	8.88	0.0033			
Serum creatinine[d]	0.210	7.23	0.0079			

ALP, alkaline phosphatase; AUC, area under concentration curve.
[a]The values after logarithmic conversion were used as an objective variable.
[b]The absolute value (g/dl) before irinotecan treatment.
[c]Grade 1 or greater scores in both serum GOT and ALP before irinotecan treatment.
[d]Grade 1 or greater scores in serum creatinine before irinotecan treatment.

Fig. 3

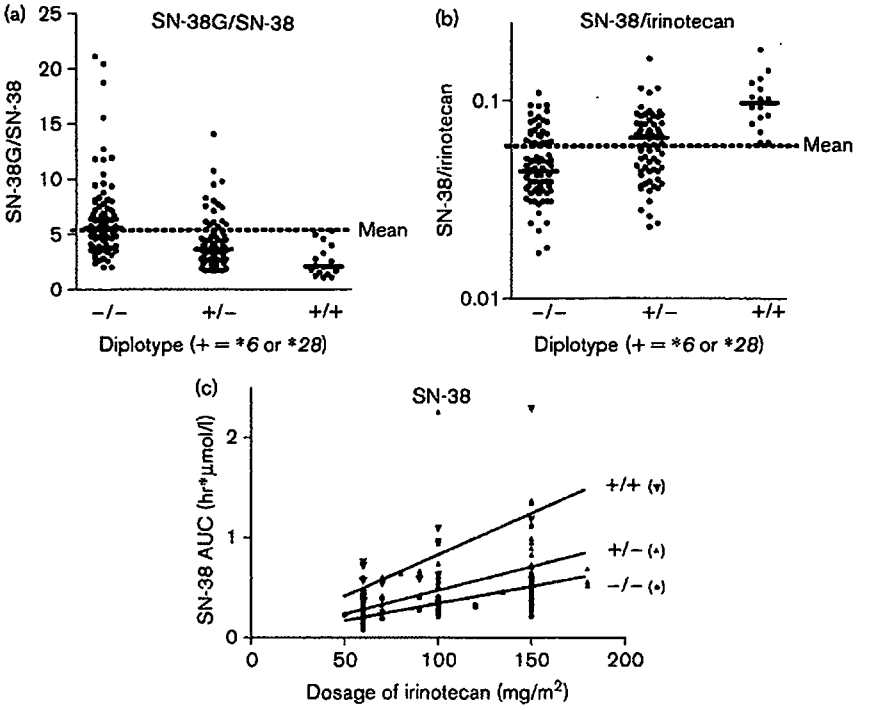

Effects of the genetic marker of *UGT1A1* '*6 or *28' on the area under concentration curve (AUC) ratios of SN-38G/SN-38 (a) and SN-38/irinotecan (b), and SN-38 by irinotecan dosage (c) in 176 Japanese cancer patients after irinotecan treatment.

Table 5 Association of *UGT1A1*6* and *28 with irinotecan toxicities

Diplotype (+ = *6 or *28)	Number of patients	Diarrhea (grade 3)	Neutropenia (grade 3 or 4)
Irinotecan monotherapy			
-/-	21	3 (14.3%)[a]	3 (14.3%)
+/-	29	2 (6.90%)	7 (24.1%)
+/+	5	1 (20.0%)	4 (80.0%)
P-value[b]		0.8500	**0.0117**
P-value[c]		0.3889	**0.0124**
With cisplatin			
-/-	35	1 (2.9%)	20 (57.1%)
+/-	20	2 (10.0%)	14 (70.0%)
+/+	7	1 (14.3%)	7 (100%)
P-value[b]		0.1747	**0.0315**
P-value[c]		0.3886	0.0863

[a]Percentage of the patient number in each diplotype is indicated in parentheses.
[b]Chi-squared test for trend.
[c]Fisher's exact test, (-/- and +/-) vs. +/+.

Table 6 Multiple regression analysis of the nadir of absolute neutrophil counts in the patients with irinotecan monotherapy

Variable	Coefficient	F-value	*P*-value	R^2	Intercept	*N*
				0.3942	643	53
Serum ALP[a]	-349.9	12.2	0.0010			
Neutrophil count before irinotecan treatment	0.2466	13.5	0.0006			
*6 or *28	-369.1	6.40	0.0146			

[a]Grade 1 or greater scores of serum ALP before irinotecan treatment.

of diarrhea in the irinotecan/capecitabine regimen, in which diarrhea was a major toxicity [20]. A highly frequent allele *1A9*22* with an insertion of T into the nine T repeats in the promoter region (-126_-118T_9 > T_{10}) was shown to have an enhanced promoter activity in an in-vitro reporter assay [21], whereas 1A9 protein expression levels did not change in the clinical samples [22]. Rare variations, *1A9*5* [766G > A(D256N)] and *UGT1A10*3* [605C > T(T202I)], were shown to cause reduced activity *in vitro*, but their clinical importance is still unknown [23,24]. Moreover, close linkages among *1A9*, *1A7*, and *1A1* polymorphisms were found in Caucasians and Asians in an ethnic-specific manner [20,25–28].

Our study also revealed close linkages between *1A9*22* and *1A7*1*, *1A7*3* and *1A1*6* or *28 [28]. This fact makes it difficult to draw firm conclusions about the effects of *1A7*3* and *1A9*22* themselves. It is, however, reasonable to conclude that the degree of neutropenia depends on the activity of UGT1A1, because UGT1A1 is a major UGT1A enzyme in the liver and plays a primary role for regulating plasma concentrations of SN-38.

Taken together, for practical application to individualized irinotecan therapy, genotyping of *UGT1A1*6* and *28 would be beneficial and necessary in Japanese cancer patients to avoid severe adverse reactions. The frequency

of homozygotes for '*6 or *28' (namely, *6/*6, *6/*28, and *28/*28) is approximately 10%, which is comparable to the frequency of *28 homozygotes in Caucasian populations. In our study, it may be difficult to establish definite guidelines for dose reductions of irinotecan for patients homozygous for '*6 or *28'. Considering, however, 2.4-fold steep relationship between the dose of irinotecan and the AUC of SN-38 for patients homozygous for '*6 or *28' compared with patients without '*6 or *28' (Fig. 3c), the dose for patients homozygous for '*6 or *28' should be reduced to a half of the dosage recommended for other patients. Prospective studies are necessary to confirm the validity of the recommendation for dose reduction in Japanese cancer patients homozygous for '*6 or *28'.

Acknowledgements

We thank Ms Chie Sudo for her secretarial assistance. This study was supported in part by the Program for the Promotion of Fundamental Studies in Health Sciences and by the Program for the Promotion of Studies in Health Sciences of the Ministry of Health, Labor and Welfare of Japan. Analytical standards of irinotecan and its metabolites were kindly supplied by Yakult Honsha Co. Ltd. (Tokyo, Japan).

References

1 Garcia-Carbonero R, Supko JG. Current perspectives on the clinical experience, pharmacology, and continued development of the camptothecins. *Clin Cancer Res* 2002; 8:641–661.
2 Slatter JG, Su P, Sams JP, Schaaf LJ, Wienkers LC. Bioactivation of the anticancer agent CPT-11 to SN-38 by human hepatic microsomal carboxylesterases and the in vitro assessment of potential drug interactions. *Drug Metab Dispos* 1997; 25:1157–1164.
3 Iyer L, King CD, Whitington PF, Green MD, Roy SK, Tephly TR, *et al.* Genetic predisposition to the metabolism of irinotecan (CPT-11). Role of uridine diphosphate glucuronosyltransferase isoform 1A1 in the glucuronidation of its active metabolite (SN-38) in human liver microsomes. *J Clin Invest* 1998; 101:847–854.
4 De Forni M, Bugat R, Chabot GG, Culine S, Extra JM, Gouyette A, *et al.* Phase I and pharmacokinetic study of the camptothecin derivative irinotecan, administered on a weekly schedule in cancer patients. *Cancer Res* 1994; 54:4347–4354.
5 Gupta E, Lestingi TM, Mick R, Ramirez J, Vokes EE, Ratain MJ. Metabolic fate of irinotecan in humans: correlation of glucuronidation with diarrhea. *Cancer Res* 1994; 54:3723–3725.
6 Hanioka N, Ozawa S, Jinno H, Ando M, Saito Y, Sawada J. Human liver UDP-glucuronosyltransferase isoforms involved in the glucuronidation of 7-ethyl-10-hydroxycamptothecin. *Xenobiotica* 2001; 31:687–699.
7 Fisher MB, VandenBranden M, Findlay K, Burchell B, Thummel KE, Hall SD, *et al.* Tissue distribution and interindividual variation in human UDP-glucuronosyltransferase activity: relationship between UGT1A1 promoter genotype and variability in a liver bank. *Pharmacogenetics* 2000; 10:727–739.
8 Ando Y, Saka H, Ando M, Sawa T, Muro K, Ueoka H, *et al.* Polymorphisms of UDP-glucuronosyltransferase gene and irinotecan toxicity: a pharmacogenetic analysis. *Cancer Res* 2000; 60:6921–6926.
9 Iyer L, Das S, Janisch L, Wen M, Ramirez J, Karrison T, *et al.* UGT1A1*28 polymorphism as a determinant of irinotecan disposition and toxicity. *Pharmacogenomics J* 2002; 2:43–47.
10 Innocenti F, Undevia SD, Iyer L, Chen PX, Das S, Kocherginsky M, *et al.* Genetic variants in the UDP-glucuronosyltransferase 1A1 gene predict the risk of severe neutropenia of irinotecan. *J Clin Oncol* 2004; 22:1382–1388.
11 Marcuello E, Altes A, Menoyo A, del Rio E, Gomez-Pardo M, Baiget M. UGT1A1 gene variations and irinotecan treatment in patients with metastatic colorectal cancer. *Br J Cancer* 2004; 91:678–682.
12 Rouits E, Boisdron-Celle M, Dumont A, Guerin O, Morel A, Gamelin E. Relevance of different UGT1A1 polymorphisms in irinotecan-induced toxicity: a molecular and clinical study of 75 patients. *Clin Cancer Res* 2004; 10:5151–5159.
13 Kaniwa N, Kurose K, Jinno H, Tanaka-Kagawa T, Saito Y, Saeki M, *et al.* Racial variability in haplotype frequencies of UGT1A1 and glucuronidation activity of a novel single nucleotide polymorphism 686C>T (P229L) found in an African-American. *Drug Metab Dispos* 2005; 33:458–465.
14 Sai K, Saeki M, Saito Y, Ozawa S, Katori N, Jinno H, *et al.* UGT1A1 haplotypes associated with reduced glucuronidation and increased serum bilirubin in irinotecan-administered Japanese patients with cancer. *Clin Pharmacol Ther* 2004; 75:501–515.
15 Ciotti M, Basu N, Brangi M, Owens IS. Glucuronidation of 7-ethyl-10-hydroxycamptothecin (SN-38) by the human UDP-glucuronosyltransferases encoded at the UGT1 locus. *Biochem Biophys Res Commun* 1999; 260:199–202.
16 Gagne JF, Montminy V, Belanger P, Journault K, Gaucher G, Guillemette C. Common human UGT1A polymorphisms and the altered metabolism of irinotecan active metabolite 7-ethyl-10-hydroxycamptothecin (SN-38). *Mol Pharmacol* 2002; 62:608–617.
17 Oguri T, Takahashi T, Miyazaki M, Isobe T, Kohno N, Mackenzie PI. UGT1A10 is responsible for SN-38 glucuronidation and its expression in human lung cancers. *Anticancer Res* 2004; 24:2893–2896.
18 Basu NK, Ciotti M, Hwang MS, Kole L, Mitra PS, Cho JW, *et al.* Differential and special properties of the major human UGT1-encoded gastrointestinal UDP-glucuronosyltransferases enhance potential to control chemical uptake. *J Biol Chem* 2004; 279:1429–1441.
19 Ando M, Ando Y, Sekido Y, Ando M, Shimokata K, Hasegawa Y. Genetic polymorphisms of the UDP-glucuronosyltransferase 1A7 gene and irinotecan toxicity in Japanese cancer patients. *Jpn J Cancer Res* 2002; 93:591–597.
20 Carlini LE, Meropol NJ, Bever J, Andria ML, Hill T, Gold P, *et al.* UGT1A7 and UGT1A9 polymorphisms predict response and toxicity in colorectal cancer patients treated with capecitabine/irinotecan. *Clin Cancer Res* 2005; 11:1226–1236.
21 Yamanaka H, Nakajima M, Katoh M, Hara Y, Tachibana O, Yamashita J, *et al.* A novel polymorphism in the promoter region of human UGT1A9 gene (UGT1A9*22) and its effects on the transcriptional activity. *Pharmacogenetics* 2004; 14:329–332.
22 Girard H, Court MH, Bernard O, Fortier LS, Villeneuve L, Hao Q, *et al.* Identification of common polymorphisms in the promoter of the UGT1A9 gene: evidence that UGT1A9 protein and activity levels are strongly genetically controlled in the liver. *Pharmacogenetics* 2004; 14:501–515.
23 Jinno H, Saeki M, Saito Y, Tanaka-Kagawa T, Hanioka N, Sai K, *et al.* Functional characterization of human UDP-glucuronosyltransferase 1A9 variant, D256N, found in Japanese cancer patients. *J Pharmacol Exp Ther* 2003; 306:688–693.
24 Jinno H, Saeki M, Tanaka-Kagawa T, Hanioka N, Saito Y, Ozawa S, *et al.* Functional characterization of wild-type and variant (T202I and M59I) human UDP-glucuronosyltransferase 1A10. *Drug Metab Dispos* 2003; 31:528–532.
25 Kohle C, Mohrle B, Munzel PA, Schwab M, Wernet D, Badary OA, *et al.* Frequent co-occurrence of the TATA box mutation associated with Gilbert's syndrome (UGT1A1*28) with other polymorphisms of the UDP-glucuronosyltransferase-1 locus (UGT1A6*2 and UGT1A7*3) in Caucasians and Egyptians. *Biochem Pharmacol* 2003; 65:1521–1527.
26 Huang MJ, Yang SS, Lin MS, Huang CS. Polymorphisms of uridine-diphosphoglucuronosyltransferase 1A7 gene in Taiwan Chinese. *World J Gastroenterol* 2005; 11:797–802.
27 Innocenti F, Liu W, Chen P, Dedai AA, Das S, Ratain MJ. Haplotypes of variants in the UDP-glucuronosyltransferase 1A9 and 1A1 genes. *Pharmacogenet Genomics* 2005; 15:295–301.
28 Saeki M, Saito Y, Jinno H, Sai K, Ozawa S, Kurose K, *et al.* Haplotype structures of the UGT1A gene complex in a Japanese population. *Pharmacogenomics J* 2006; 6:63–75.
29 Sai K, Kaniwa N, Ozawa S, Sawada J. An analytical method for irinotecan (CPT-11) and its metabolites using a high-performance liquid chromatography: parallel detection with fluorescence and mass spectrometry. *Biomed Chromatogr* 2002; 16:209–218.
30 Benjamini Y, Hochberg Y. Controlling the false discovery rate: a practical and powerful approach to multiple testing. *J Roy Stat Soc B* 1995; 57:289–300.
31 Han JY, Lim HS, Shin ES, Yoo YK, Park YH, Lee JE, *et al.* Comprehensive analysis of UGT1A polymorphisms predictive for pharmacokinetics and treatment outcome in patients with non-small-cell lung cancer treated with irinotecan and cisplatin. *J Clin Oncol* 2006; 24:2237–2244.
32 Kitagawa C, Ando M, Ando Y, Sekido Y, Wakai K, Imaizumi K, *et al.* Genetic polymorphism in the phenobarbital-responsive enhancer module of the UDP-glucuronosyltransferase 1A1 gene and irinotecan toxicity. *Pharmacogenet Genomics* 2005; 15:35–41.

Large Cell Neuroendocrine Carcinoma of the Mediastinum with α-Fetoprotein Production

Ken Takezawa, MD, Isamu Okamoto, MD, PhD,* Junya Fukuoka, MD, PhD,† Kaoru Tanaka, MD,* Hiroyasu Kaneda, MD,* Hisao Uejima, MD,‡ Hyung-Eun Yoon, MD, PhD,‡ Masami Imakita, MD, PhD,§ Masahiro Fukuoka, MD, PhD,* and Kazuhiko Nakagawa, MD, PhD**

Large cell neuroendocrine carcinoma (LCNEC) is a relatively new category of pulmonary neuroendocrine tumor. Although it was first detected in the lung, LCNEC has since been found in a variety of extrapulmonary sites. We now describe a patient who was diagnosed with LCNEC originating from the mediastinum, an extremely rare disorder. An increased serum concentration of α-fetoprotein (AFP) in the patient was reduced by chemotherapy in association with tumor shrinkage. Furthermore, the tumor was confirmed immunohistochemically to produce AFP. To our knowledge, this is the first report of a LCNEC that produces AFP.

Key Words: Large cell neuroendocrine carcinoma, α-Fetoprotein, Mediastinal tumor.

(*J Thorac Oncol.* 2008;3: 187–189)

Large cell neuroendocrine carcinoma (LCNEC) is a high-grade neuroendocrine tumor that was first detected in the lung by Travis et al.[1] The prognosis of individuals with LCNEC has been reported to be poor, with a 5-year survival rate similar to that for small cell carcinoma.[2–4] Although originally found in the lung, LCNEC has since been described in a variety of extrapulmonary locations.[5–7] Among these locations, mediastinal LCNEC is extremely rare, with only a few cases having been reported.[8,9] We now report the first case of mediastinal LCNEC with α-fetoprotein (AFP) production.

CASE REPORT

A previously healthy 35-year-old Japanese man was found to have an abnormal mass in his right mediastinum on a chest radiograph during a health checkup. The patient's general condition was fair, and symptoms such as chest pain, weight loss, or fever were not noted. He was a current smoker, having smoked 20 cigarettes a day for 15 years. Computed tomography imaging of the chest revealed a 65 × 50 mm mass in the middle mediastinum (Figure 1*A*). Serum laboratory data were within normal limits. A bronchoscopic examination revealed a compression against the outside of the trachea. No other organs appeared to be affected on extensive examination. Subsequent evaluation for serum tumor markers revealed an increased level of AFP. Other examined markers, including β-human chorionic gonadotropin, carcinoembryonic antigen, and CA19-9, were within normal limits. Thoracoscopic examination revealed that the tumor was not invading into the adjacent lung. On the basis of these findings, we considered the tumor to have originated from the middle mediastinum. A biopsy revealed poorly differentiated carcinoma with neuroendocrine features. Thymic neuroendocrine carcinoma is exclusively located in the anterior-superior mediastinum.[1] Given the tumor's location, the increase in the serum concentration of AFP, and the patient's young age, the diagnosis of embryonal carcinoma was initially favored over purely neuroendocrine neoplasm. The patient received neoadjuvant chemotherapy with bleomycin (30 mg/body) on days 2, 9, and 16, etoposide (100 mg/m^2) on days 1 to 5, and cisplatin (20 mg/m^2) on days 1 to 5. Treatment cycles were repeated every 21 days for 4 cycles. The serum AFP level had decreased to within normal limits in association with shrinkage of the tumor by the end of the third cycle of chemotherapy (Figure 1*B*, *E*). However, the AFP concentration started to increase thereafter, and progression of the tumor was confirmed after the fourth cycle of chemotherapy (Figure 1*C*, *E*). The patient then received second-line chemotherapy with cisplatin (80 mg/m^2) on day 1 and paclitaxel (200 mg/m^2) on day 1 every 21 days for three cycles before surgery. The serum AFP level again decreased in association with tumor shrinkage (Figure 1*D*, *E*). Eight months after initial detection of the tumor, the patient underwent a tumorectomy combined with right upper lobectomy and tracheoplasty, given that the tumor was found to invade the adjacent right upper lobe and trachea at the time of surgery. Histopathologic examination of the surgical specimen revealed a solid tumor nest with massive necrosis. The tumor was relatively homogeneous throughout the resection, showing sheets of cells with a high nucleus-to-cytoplasm ratio. High-power magnification of the tumor revealed that the tumor cells manifested marked neu-

*Department of Medical Oncology, Kinki University School of Medicine, Osaka; †Laboratory of Pathology, Toyama University Hospital, Toyama; ‡Division of Respirology; and §Division of Pathology, Rinku General Medical Center, Osaka, Japan.

Disclosure: The authors declare no conflict of interest.

Address for correspondence: Isamu Okamoto, MD, PhD, Department of Medical Oncology, Kinki University School of Medicine, 377-2 Ohno-higashi, Osaka-Sayama, Osaka 589-8511. E-mail: chi-okamoto@dotd.med.kindai.ac.jp

Copyright © 2008 by the International Association for the Study of Lung Cancer

ISSN: 1556-0864/08/0302-0187

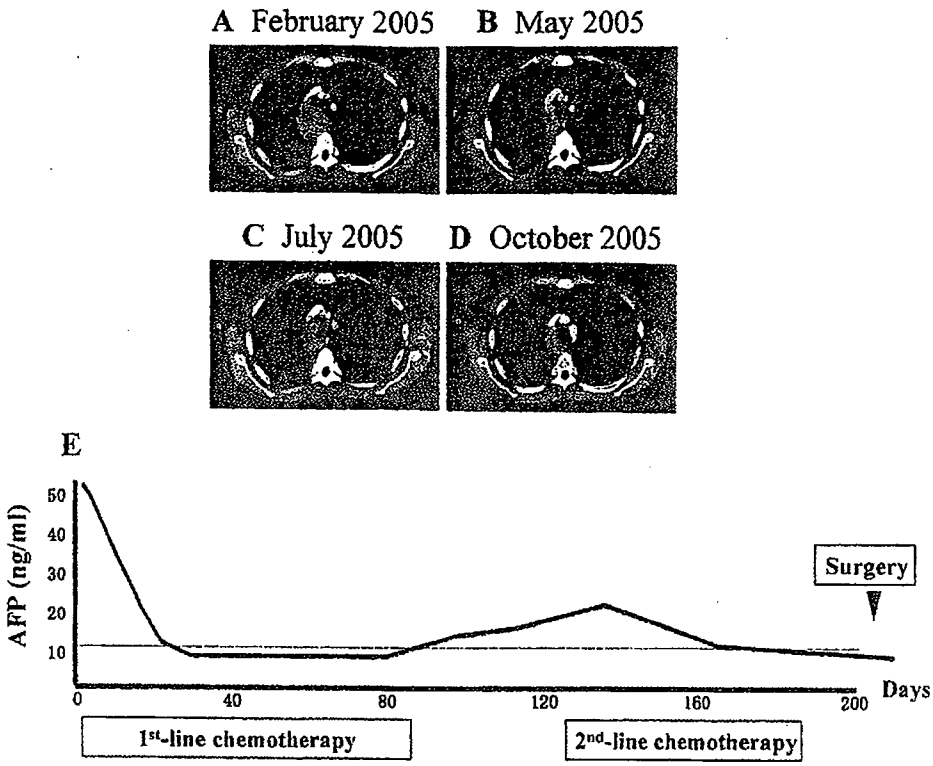

FIGURE 1. Chest computed tomography (CT) findings and serum AFP levels in the patient. *A–D*, Chest CT findings. A mass in the middle mediastinum was initially detected (*A*). The tumor had shrunk after three cycles of neoadjuvant chemotherapy (*B*), but its progression had resumed after the fourth cycle (*C*). The tumor shrank again in response to second-line chemotherapy (*D*). *E*, Time course of the serum concentration of AFP. The AFP level was initially increased, it decreased to within normal limits (dotted line) in association with tumor shrinkage during first-line chemotherapy, but it started to increase again after the third cycle. The serum AFP level again decreased in association with tumor shrinkage during second-line chemotherapy.

roendocrine features, such as frequent rosette structures and trabecular arrangements, nuclear moldings, and prominent mitoses (Figure 2*A*, *B*). The tumor cells also had abundant nucleoli. Immunohistochemical analysis showed the tumor cells to be diffusely positive for CK7 and neuroendocrine markers including CD56, chromogranin A (Figure 2*C*), and synaptophysin as well as negative for CD5, CD30, human chorionic gonadotropin, placental alkaline phosphatase, hepatocyte antigen, and thyroid transcription factor-1. No regions of the specimen showed features of a germ cell tumor or hepatoid carcinoma. On the basis of the morphology and staining characteristics of the tumor, a pathologic diagnosis of LCNEC was made. A small number of tumor cells showed subtle but unequivocal positive staining for AFP (Figure 2*D*). Thoracic radiotherapy was not able to be given because the patient suffered from thoracic empyema after surgery. Despite intensive chemotherapy, he died of extensive recurrence of carcinoma 4 months after the surgery.

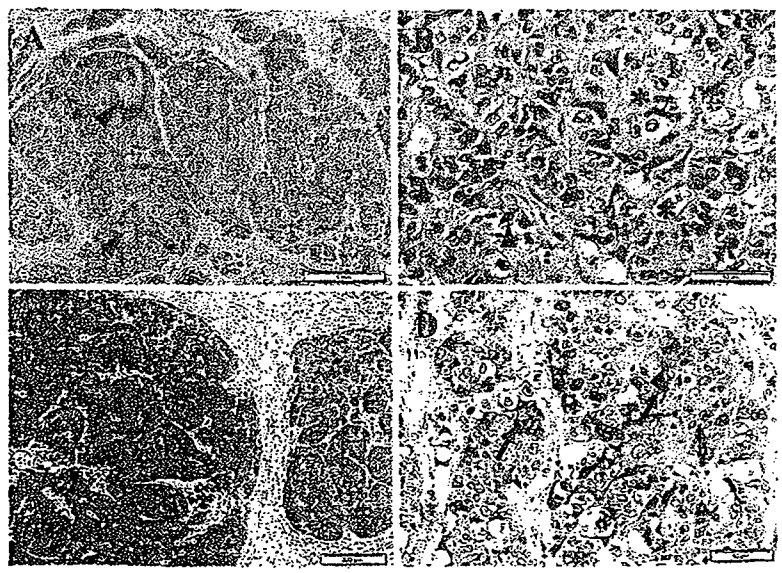

FIGURE 2. Histology and immunohistochemical analysis of the tumor specimen obtained at surgery. *A*, Hematoxylin-eosin staining revealed solid tumor nests with areas of necrosis (arrow heads). Note the homogeneous appearance of the tumor. *B*, High-power magnification of the tumor stained as in (*A*), showing numerous rosettes (asterisk), abundant cytoplasm, chromatin clearing with occasionally prominent nucleoli, nuclear molding (arrows), and frequent mitosis (arrow heads). *C*, Immunohistochemical staining for chromogranin A revealed diffuse and intense cytoplasmic staining. *D*, Immunohistochemical staining for AFP, showing a focus of tumor cells positive for AFP (arrows). Scale bars: 1 mm, 50 μ.

Copyright © 2008 by the International Association for the Study of Lung Cancer

DISCUSSION

LCNEC is a relatively new category of pulmonary neuroendocrine tumor, with affected individuals reported to have a prognosis intermediate between those with atypical carcinoid lung cancer and those with small cell lung cancer.[10] Recent clinical studies indicate a 5-year survival rate of 27 to 67% even if patients are at pathologic stage I.[2–4] Since its original detection in the lung, LCNEC has been found in a variety of extrapulmonary locations including gastrointestinal sites and the uterine cervix.[5–7] The present case was identified as LCNEC originating in the mediastinum. Given the age of the patient and the tumor location, a diagnosis of embryonal carcinoma was initially considered, but no morphologic or immunohistochemical features indicative of embryonal carcinoma were found on extensive pathologic analysis of the surgical specimen. Primary mediastinal LCNEC is an extremely rare disorder and has been described in only a few case reports to date.[8–9]

In the present case, the increased serum AFP level decreased in association with tumor shrinkage in response to chemotherapy, and the tumor was confirmed immunohistochemically to produce AFP. AFP is the main component of fetal serum in mammals. It is synthesized by visceral endoderm of the yolk sac and fetal liver, but expression of the *AFP* gene is greatly reduced at the time of birth. AFP-producing carcinoma has been recognized for decades and reported in various locations including the lung and mediastinum.[11] In contrast to the present case, however, most cancers that produce AFP show morphologic features similar to hepatocellular carcinoma. With regard to neuroendocrine tumors, some case reports indicate that small cell carcinoma can also produce AFP.[12,13] As far as we are aware, however, the present case is the first reported example of LCNEC producing AFP. Given that the concept of LCNEC is relatively new, this may not be that surprising, and previous reports of small cell carcinoma may actually have been diagnosed as LCNEC today. Our case raises the possibility that the origin of mediastinal neuroendocrine tumors including LCNEC may be mediastinal primordial germ cells. Examination of germ cell tumor markers in neuroendocrine tumors may shed light on this matter.

REFERENCES

1. Travis WD, Linnoila RI, Tsokos MG, et al. Neuroendocrine tumors of the lung with proposed criteria for large-cell neuroendocrine carcinoma. An ultrastructural, immunohistochemical, and flow cytometric study of 35 cases. *Am J Surg Pathol* 1991;15:529–553.
2. Iyoda A, Hiroshima K, Toyozaki T, et al. Clinical characterization of pulmonary large cell neuroendocrine carcinoma and large cell carcinoma with neuroendocrine morphology. *Cancer* 2001;91:1992–2000.
3. Takei H, Asamura H, Maeshima A, et al. Large cell neuroendocrine carcinoma of the lung: a clinicopathologic study of eighty-seven cases. *J Thorac Cardiovasc Surg* 2002;124:285–292.
4. Travis WD, Rush W, Flieder DB, et al. Survival analysis of 200 pulmonary neuroendocrine tumors with clarification of criteria for atypical carcinoid and its separation from typical carcinoid. *Am J Surg Pathol* 1998;22:934–944.
5. Jiang SX, Mikami T, Umezawa A, et al. Gastric large cell neuroendocrine carcinomas: a distinct clinicopathologic entity. *Am J Surg Pathol* 2006;30:945–953.
6. Selvakumar E, Vimalraj V, Rajendran S, et al. Large cell neuroendocrine carcinoma of the ampulla of Vater. *Hepatobiliary Pancreat Dis Int* 2006;5:465–467.
7. Tangjitgamol S, Manusirivithaya S, Choomchuay N, et al. Paclitaxel and carboplatin for large cell neuroendocrine carcinoma of the uterine cervix. *J Obstet Gynaecol Res* 2007;33:218–224.
8. Chetty R, Batitang S, Govender D. Large cell neuroendocrine carcinoma of the thymus. *Histopathology* 1997;31:274–276.
9. Nagata Y, Ohno K, Utsumi T, et al. Large cell neuroendocrine thymic carcinoma coexisting within large WHO type AB thymoma. *Jpn J Thorac Cardiovasc Surg* 2006;54:256–259.
10. Moran CA, Suster S. Neuroendocrine carcinomas (carcinoid tumor) of the thymus. A clinicopathologic analysis of 80 cases. *Am J Clin Pathol* 2000;114:100–110.
11. Nasu M, Soma T, Fukushima H, et al. Hepatoid carcinoma of the lung with production of alpha-fetoprotein and abnormal prothrombin: an autopsy case report. *Mod Pathol* 1997;10:1054–1058.
12. Morikawa T, Kobayashi S, Yamadori I, et al. Three cases of extrapulmonary small cell carcinoma occurring in the prostate, stomach, and pancreas. *Indian J Cancer* 1994;31:268–273.
13. Yamaguchi T, Imamura Y, Nakayama K, et al. Paranuclear blue inclusions of small cell carcinoma of the stomach: report of a case with cytologic presentation in peritoneal washings. *Acta Cytol* 2005;49:207–212.

Copyright © 2008 by the International Association for the Study of Lung Cancer

Int. J. Cancer: **122**, 1530–1538 (2008)
© 2007 Wiley-Liss, Inc.

Matuzumab and cetuximab activate the epidermal growth factor receptor but fail to trigger downstream signaling by Akt or Erk

Takeshi Yoshida[1], Isamu Okamoto[1]*, Takafumi Okabe[1], Tsutomu Iwasa[1], Taroh Satoh[1], Kazuto Nishio[2], Masahiro Fukuoka[3] and Kazuhiko Nakagawa[1]

[1]*Department of Medical Oncology, Kinki University School of Medicine, Osaka, Japan*
[2]*Department of Genome Biology, Kinki University School of Medicine, Osaka, Japan*
[3]*Sakai Hospital, Kinki University School of Medicine, Osaka, Japan*

Molecular inhibition of the epidermal growth factor receptor (EGFR) is a promising anticancer strategy, and monoclonal antibodies (mAbs) to EGFR are undergoing extensive evaluation in preclinical and clinical trials. However, the effects of anti-EGFR mAbs on EGFR signaling have remained unclear. We have now examined the effects of 2 anti-EGFR mAbs, matuzumab (EMD72000) and cetuximab (Erbitux), both of which are currently under assessment for treatment of various cancers, on EGFR signal transduction and cell survival in nonsmall cell lung cancer cell lines. Similar to EGF, matuzumab and cetuximab each induced phosphorylation of EGFR at several tyrosine phosphorylation sites as a result of receptor dimerization and activation of the receptor tyrosine kinase. In contrast to the effects of EGF, however, EGFR activation induced by these antibodies was not accompanied by receptor turnover or by activation of downstream signaling pathways that are mediated by Akt and Erk and are important for regulation of cell proliferation and survival. In addition, clonogenic survival assays revealed that matuzumab and cetuximab reduced the survival rate of H292 cells, in which they also inhibited the EGF-induced activation of Akt and Erk. Although we have examined only a few cell lines, our results indicate that the antitumor effects of matuzumab and cetuximab depend on inhibition of EGFR downstream signaling mediated by Akt or Erk rather than on inhibition of EGFR itself.
© *2007 Wiley-Liss, Inc.*

Key words: EGF receptor; signal transduction; matuzumab; cetuximab; nonsmall cell lung cancer

The epidermal growth factor receptor (EGFR, also known as ErbB1), a member of the ErbB family of receptor tyrosine kinases, is a 170-kDa plasma membrane glycoprotein composed of an extracellular ligand binding domain, a transmembrane region and an intracellular tyrosine kinase domain with a regulatory COOH-terminal segment.[1] Binding of ligand to EGFR induces receptor dimerization, activation of the receptor kinase and autophosphorylation of specific tyrosine residues within the COOH-terminal region of the protein.[1] These events trigger intracellular signaling pathways that promote cell proliferation and survival.[2,3]

EGFR is frequently overexpressed in many types of human malignancy, with the extent of overexpression being negatively correlated with prognosis.[4,5] Recognition of the role of EGFR in carcinogenesis has prompted the development of EGFR-targeted therapies that include both small-molecule tyrosine kinase inhibitors (TKIs) that target the intracellular tyrosine kinase domain and monoclonal antibodies (mAbs) that target the extracellular domain.[6–8] Among EGFR-TKIs, gefitinib and erlotinib have been extensively evaluated in nonsmall cell lung cancer (NSCLC), and sensitivity to these drugs has been correlated with the presence of somatic mutations in the EGFR kinase domain or with EGFR gene (*EGFR*) amplification.[9–16] Among anti-EGFR mAbs, cetuximab (Erbitux), a chimeric mouse-human antibody of the immunoglobulin (Ig) G1 subclass, has proved efficacious in the treatment of irinotecan-refractory colon cancer[17] and was recently approved by the U.S. Food and Drug Administration for the treatment of patients with head and neck squamous cell carcinoma.[18] Several clinical studies of anti-EGFR mAbs such as matuzumab (EMD72000, humanized IgG1) and cetuximab are ongoing for other types of cancer including NSCLC.[19–24] Anti-EGFR mAbs bind to the extracellular ligand binding domain of the receptor and are thereby thought to block ligand binding.[18,25] The antitumor effects of these mAbs are thus thought to be attributable to inhibition of EGFR signaling as well as to other mechanisms such as antibody-dependent cellular cytotoxicity.[18,26] However, the detailed effects of anti-EGFR mAbs on EGFR signaling have remained unclear.[27–30]

We have now examined in detail the effects on EGFR signal transduction of 2 anti-EGFR mAbs, matuzumab and cetuximab, both of which are used clinically, to provide insight into the mechanisms of their antitumor effects.

Material and methods

Cell culture and reagents

The human NSCLC cell lines NCI-H292 (H292), NCI-H460 (H460) and Ma-1 were obtained as previously described[31] and were cultured under a humidified atmosphere of 5% CO_2 at 37°C in RPMI 1640 medium (Sigma, St. Louis, MO) supplemented with 10% fetal bovine serum. Matuzumab and cetuximab were kindly provided by Merck KGaA (Darmstadt, Germany) and Bristol Myers (New York, NY), respectively; gefitinib was obtained from AstraZeneca (Macclesfield, UK); and trastuzumab (Herceptin; Genentech, South San Francisco, CA) was obtained from Chugai (Tokyo, Japan). Neutralizing antibodies to EGFR (clone LA1) were obtained from Upstate Biotechnology (Lake Placid, NY).

Immunoblot analysis

Cell lysates were fractionated by SDS-polyacrylamide gel electrophoresis on a 7.5% gel, and the separated proteins were transferred to a nitrocellulose membrane. After blocking of nonspecific sites, the membrane was incubated consecutively with primary and secondary antibodies, and immune complexes were detected with the use of enhanced chemiluminescence reagents, as described previously.[31] Primary antibodies to the specific intracellular phosphorylation sites of EGFR (pY845, pY1068 or pY1173), to Erk, to phospho-Akt and to Akt were obtained from Cell Signaling Technology (Beverly, MA); those to the extracellular domain of EGFR (clone 31G7) were from Zymed (South San Francisco, CA); those to the intracellular domain of EGFR (EGFR 1005) and to phospho-Erk were from Santa Cruz Biotechnology (Santa Cruz, CA); and those to β-actin (loading control) were from Sigma. Horseradish peroxidase-conjugated goat antibodies to mouse or rabbit IgG were obtained from Amersham Biosciences (Little Chalfont, UK).

Chemical cross-linking assay

Cells were incubated first with 1 mM bis(sulfosuccinimidyl) suberate (BS^3; Pierce, Rockford, IL) for 20 min at 4°C and then with

Abbreviations: EGFR, epidermal growth factor receptor; TKI, tyrosine kinase inhibitor; mAb, monoclonal antibody; NSCLC, nonsmall cell lung cancer; Ig, immunoglobulin; BS^3, bis(sulfosuccinimidyl) suberate; PE, R-phycoerythrin; PI3K, phosphoinositide 3-kinase.

***Correspondence to:** Department of Medical Oncology, Kinki University School of Medicine, 377-2 Ohno-higashi, Osaka-Sayama, Osaka 589-8511, Japan. Fax: +81-72-360-5000.
E-mail: chi-okamoto@dotd.med.kindai.ac.jp
Received 7 June 2007; Accepted after revision 26 September 2007
DOI 10.1002/ijc.23253
Published online 21 November 2007 in Wiley InterScience (www.interscience.wiley.com).

UICC Publication of the International Union Against Cancer

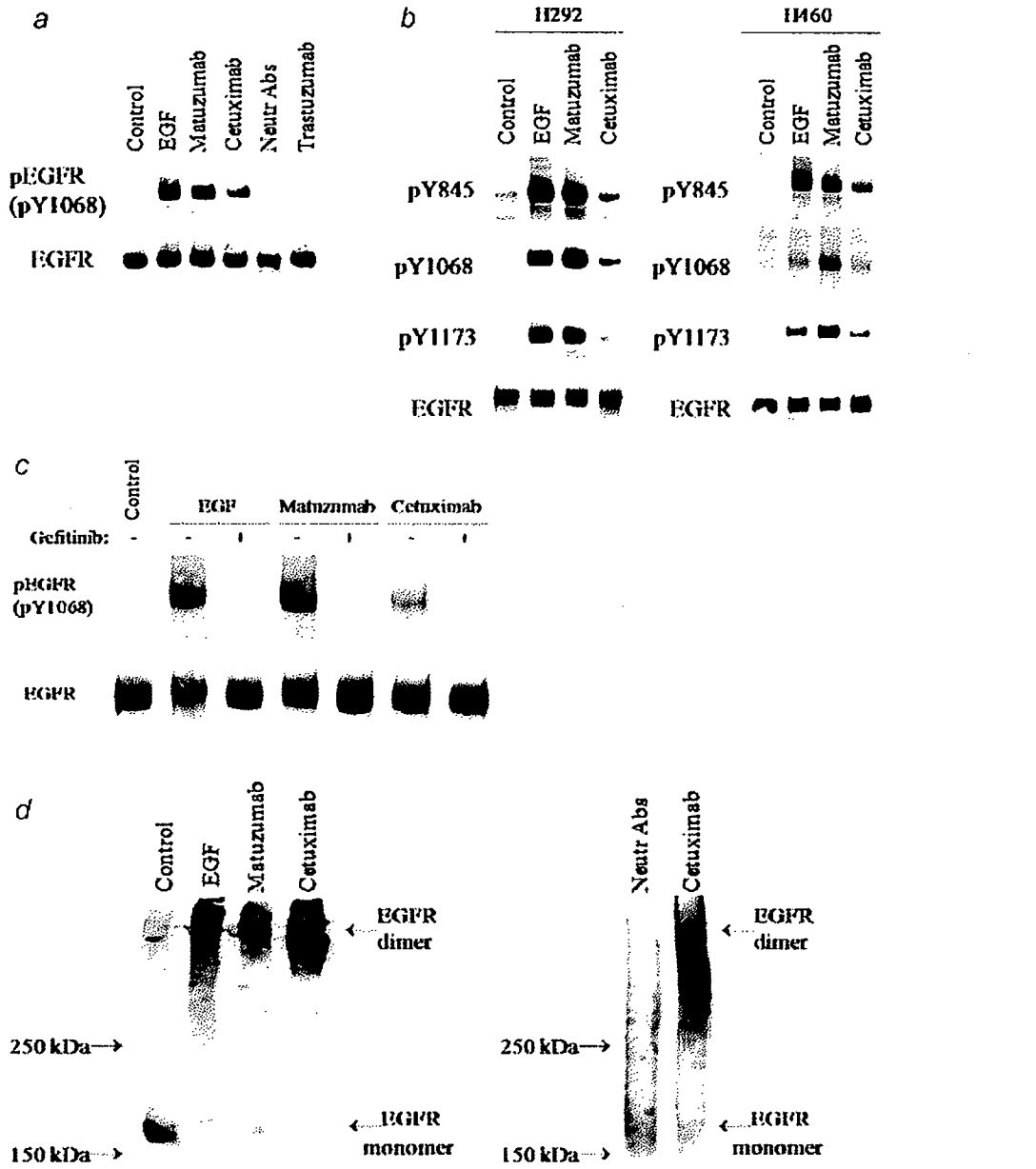

FIGURE 1 – EGFR phosphorylation induced by matuzumab or cetuximab as a result of receptor dimerization and activation of the receptor tyrosine kinase. (*a*) H292 cells were deprived of serum overnight and then incubated for 15 min in the absence (Control) or presence of matuzumab (200 nM), cetuximab (100 nM), neutralizing antibodies to EGFR (80 nM), trastuzumab (50 nM) or EGF (100 ng/ml). Cell lysates were subjected to immunoblot analysis with antibodies to the Y1068-phosphorylated form of EGFR (pY1068) and to total EGFR (the extracellular domain). (*b*) H292 or H460 cells were deprived of serum overnight and then incubated for 15 min in the absence or presence of matuzumab (200 nM), cetuximab (100 nM) or EGF (100 ng/ml). Cell lysates were subjected to immunoblot analysis with antibodies to the Y845-, Y1068- or Y1173-phosphorylated forms of EGFR and to total EGFR (the extracellular domain). (*c*) H292 cells were deprived of serum overnight and then incubated for 15 min in the absence or presence of matuzumab (200 nM), cetuximab (100 nM), EGF (100 ng/ml) or gefitinib (10 μM), as indicated. Cell lysates were subjected to immunoblot analysis with antibodies to the Y1068-phosphorylated form of EGFR and to total EGFR (the extracellular domain). (*d*) H292 cells were deprived of serum overnight and then incubated for 15 min in the absence or presence of matuzumab (200 nM), cetuximab (100 nM), neutralizing antibodies to EGFR (80 nM) or EGF (100 ng/ml). The cells were then washed and exposed to the chemical cross-linker BS^3 after which cell lysates were subjected to immunoblot analysis with antibodies to EGFR (the intracellular domain). The positions of EGFR monomers and dimers as well as of molecular size standards are indicated.

250 mM glycine for 5 min at 4°C to terminate the cross-linking reaction, as described previously.[31] Cell lysates were resolved by SDS-polyacrylamide gel electrophoresis on a 4% gel and subjected to immunoblot analysis with rabbit polyclonal antibodies to the intracellular domain of EGFR (EGFR 1005).

Immunofluorescence analysis

Cells were grown to 50% confluence in 2-well Lab-Tec Chamber Slides (Nunc, Naperville, IL), deprived of serum overnight, and then incubated with 200 nM matuzumab or EGF (100 ng/ml) for 4 hr at 37°C. They were fixed with 4% paraformaldehyde for

30 min at 4°C, permeabilized with 0.1% Triton X-100 for 10 min, and exposed to 5% nonfat dried milk for 1 hr at room temperature. The cells were stained with rabbit polyclonal antibodies to the intracellular domain of EGFR (EGFR 1005) for 1 hr at room temperature and then incubated for an additional 45 min with Alexa 488-labeled goat antibodies to rabbit IgG (Molecular Probes, Eugene, OR). Cell nuclei were counterstained for 5 min at room temperature with 4′,6-diamidino-2-phenylindole (Sigma) at 2 μg/ml. The chamber slides were mounted in fluorescence mounting medium (DakoCytomation, Hamburg, Germany), and fluorescence signals were visualized with a fluorescence microscope (Eclipse E800; Nikon, Kawasaki, Japan). Negative controls (secondary antibodies alone) did not yield any substantial background staining.

Flow cytometry

Cells were deprived of serum overnight and then incubated with 200 nM matuzumab or EGF (100 ng/ml) for 4 hr at 37°C. They were isolated by exposure to trypsin, and aliquots of ~1.0 × 10^6 cells were incubated for 2 hr at 4°C either with an R-phycoerythrin (PE)-conjugated mouse mAb to EGFR (clone EGFR.1; Becton Dickinson, San Jose, CA), which does not interfere with the binding of EGF to EGFR,[32] or with a PE-conjugated isotype-matched control mAb (Becton Dickinson). The cells were then examined by flow cytometry (FACScalibur, Becton Dickinson) to detect the intensity of EGFR staining at the cell surface.

Clonogenic assay

Cells were plated in triplicate at a density of 200 per 25-cm^2 flask containing 10 ml of medium and were cultured for 7 days in the presence of the indicated concentrations of matuzumab or cetuximab. They were then incubated in medium alone for 7 days at 37°C, fixed with methanol:acetic acid (10:1, v/v), and stained with crystal violet. Colonies containing >50 cells were counted for calculation of the surviving fraction as follows: (mean number of colonies)/(number of inoculated cells × plating efficiency). Plating efficiency was defined as the mean number of colonies divided by the number of inoculated cells for untreated controls.

Results

Matuzumab and cetuximab induce EGFR phosphorylation in a manner dependent on the receptor tyrosine kinase activity

With the use of immunoblot analysis, we first examined the effects of the anti-EGFR mAbs matuzumab and cetuximab on EGFR phosphorylation in human NSCLC H292 cells, which express wild-type EGFR. Incubation of the serum-deprived cells for 15 min with EGF, matuzumab or cetuximab-induced phosphorylation of EGFR on tyrosine-1068 (Y1068), whereas treatment of the cells with neutralizing antibodies to EGFR or with trastuzumab, a mAb specific for HER2 (ErbB2), had no such effect (Fig. 1*a*). Furthermore, like EGF, matuzumab and cetuximab each induced phosphorylation of EGFR on Y845, Y1068 and Y1173 in H292 and H460 cells (Fig. 1*b*), the latter of which are also human NSCLC cells that express wild-type EGFR.

To determine whether the antibody-induced phosphorylation of EGFR requires the kinase activity of the receptor, we examined the effect of gefitinib, a specific EGFR-TKI. H292 cells were deprived of serum and then exposed to matuzumab, cetuximab or EGF for 15 min in the absence or presence of gefitinib. EGFR phosphorylation on Y1068 induced by EGF, matuzumab or cetuximab was completely blocked by gefitinib (Fig. 1*c*). These findings thus indicated that, like EGF, matuzumab and cetuximab each induce EGFR phosphorylation by activating the tyrosine kinase of the receptor.

Matuzumab and cetuximab induce EGFR dimerization

Ligand-dependent EGFR dimerization is responsible for activation of the receptor tyrosine kinase.[33,34] To examine whether matuzumab or cetuximab induces EGFR dimerization, we incubated serum-deprived H292 cells with the mAbs for 15 min and then exposed the cells to the chemical cross-linker BS^3. Immunoblot analysis of cell lysates with antibodies to the intracellular domain of EGFR revealed that matuzumab and cetuximab each induced EGFR dimerization to an extent similar to that observed with EGF, whereas only the monomeric form of the receptor was detected in control cells or in cells treated with neutralizing antibodies to EGFR (Fig. 1*d*). These data thus suggested that matuzumab and cetuximab activate EGFR through induction of receptor dimerization.

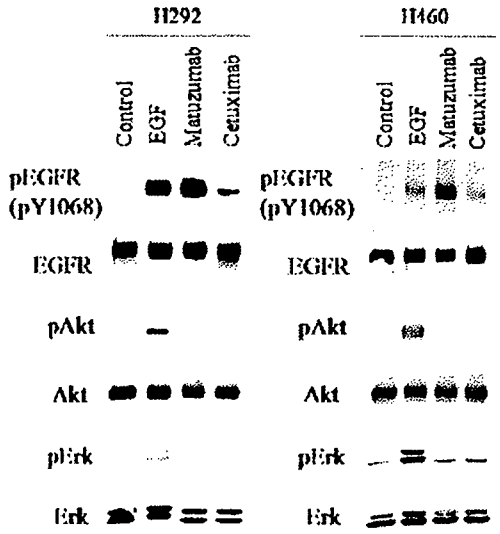

FIGURE 2 – Failure of matuzumab or cetuximab to activate Akt or Erk. H292 or H460 cells were deprived of serum overnight and then incubated for 15 min in the absence or presence of matuzumab (200 nM), cetuximab (100 nM) or EGF (100 ng/ml). Cell lysates were subjected to immunoblot analysis with antibodies to the Y1068-phosphorylated form of EGFR, to phosphorylated Akt and to phosphorylated Erk as well as with antibodies to total EGFR (the extracellular domain), Akt or Erk.

Matuzumab and cetuximab fail to induce signaling downstream of EGFR

EGFR signaling is transduced by 2 main pathways mediated by phosphoinositide 3-kinase (PI3K) and Akt and by Ras, Raf and Erk.[35,36] To determine whether EGFR phosphorylation induced by matuzumab or cetuximab is accompanied by activation of these pathways, we examined the levels of phosphorylated (activated) Akt and Erk in H292 and H460 cells treated with these antibodies for 15 min after serum deprivation. In contrast to the effects of EGF, neither matuzumab nor cetuximab induced the phosphorylation of Akt or Erk in H292 or H460 cells (Fig. 2). These results thus indicated that matuzumab and cetuximab induce EGFR activation but fail to activate the downstream Akt and Erk signaling pathways.

Matuzumab and cetuximab do not induce EGFR downregulation

Endocytic trafficking of EGFR is important for full activation of Erk and PI3K.[37] To examine further the defect in signaling downstream of EGFR activation by matuzumab or cetuximab, we determined the effects of these mAbs on receptor turnover. H292 or H460 cells were deprived of serum and then cultured with EGF, matuzumab or cetuximab for various times up to 24 hr, after which the levels of phosphorylated and total EGFR, Akt and Erk were measured. In both H292 and H460 cells treated with EGF, the amount of total EGFR decreased in a time-dependent manner

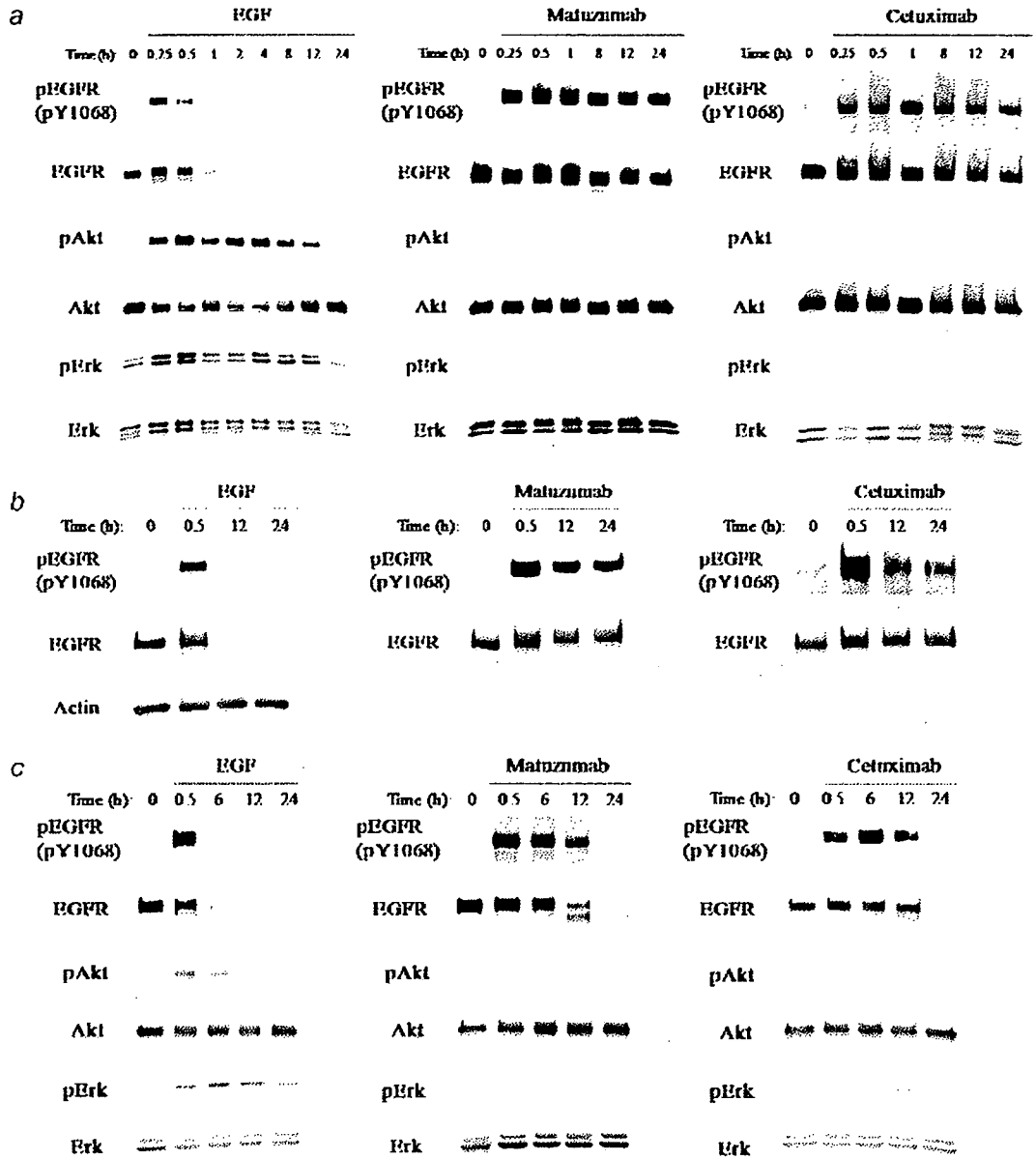

FIGURE 3 – Lack of EGFR turnover in cells treated with matuzumab or cetuximab. (*a*) H292 cells were deprived of serum overnight and then incubated for the indicated times in the presence of EGF (100 ng/ml), matuzumab (200 nM) or cetuximab (100 nM), respectively. Cell lysates were subjected to immunoblot analysis with antibodies to phosphorylated forms of EGFR (pY1068), Akt or Erk as well as with those to total EGFR (the extracellular domain), Akt or Erk. (*b*) H292 cells deprived of serum overnight were incubated for the indicated times in the presence of EGF (100 ng/ml), matuzumab (200 nM) or cetuximab (100 nM). Cell lysates were subjected to immunoblot analysis with antibodies to theY1068-phosphorylated form of EGFR, to total EGFR (the intracellular domain) or to β-actin (loading control). (*c*) H460 cells deprived of serum overnight were incubated for the indicated times in the presence of EGF (100 ng/ml), matuzumab (200 nM) or cetuximab (100 nM), after which cell lysates were subjected to immunoblot analysis with antibodies to phosphorylated forms of EGFR (pY1068), Akt or Erk as well as with those to total EGFR (the intracellular domain), Akt or Erk. (*d*) H292 cells plated on chamber slides were deprived of serum overnight and then incubated for 4 hr in the absence or presence of matuzumab (200 nM) or EGF (100 ng/ml). The cells were fixed, permeabilized, and stained with antibodies to EGFR and Alexa 488-labeled secondary antibodies (green). Cell nuclei were counterstained with 4′,6-diamidino-2-phenylindole (blue). Fluorescence signals were visualized with a fluorescence microscope, and the merged images are shown. Scale bar, 20 μm. (*e*) H292 cells were deprived of serum overnight and then incubated for 4 hr in the absence or presence of matuzumab (200 nM) or EGF (100 ng/ml). The cells were stained with either a PE-conjugated mAb to EGFR (right peaks) or a PE-labeled isotype-matched mAb (left peaks) and analyzed by flow cytometry. Representative histograms of relative cell number versus PE fluorescence are shown.

(Figs. 3*a*–3*c*), an effect that has been shown to be the result of receptor internalization and degradation.[30,38] In parallel with this EGFR downregulation, the extent of EGF-induced tyrosine phosphorylation of EGFR also decreased and was virtually undetectable by 4–6 hr (Figs. 3*a*–3*c*). The phosphorylation of Akt and Erk induced by EGF persisted for at least 12 hr but had declined by 24 hr in both cell lines (Figs. 3*a* and 3*c*). In contrast, the levels of phosphorylated and total EGFR in H292 cells treated with

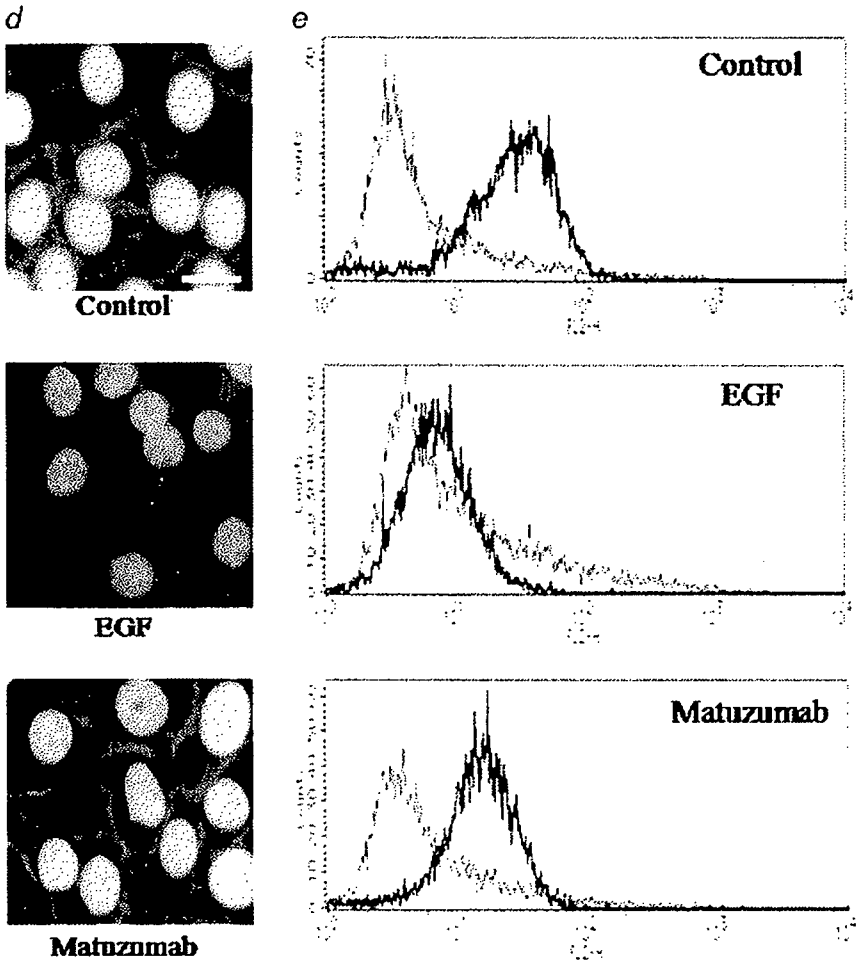

FIGURE 3 – CONTINUED

matuzumab or cetuximab for 24 hr were similar to those apparent after exposure to the antibodies for only 15 or 30 min (Figs. 3*a* and 3*b*). A marked delay in EGFR turnover was also apparent in H460 cells treated with matuzumab or cetuximab (Fig. 3*c*), although EGFR dephosphorylation and downregulation had occurred by 24 hr. Neither matuzumab nor cetuximab induced the activation of Akt or Erk or affected the total amounts of these proteins over a period of 24 hr in either cell line (Figs. 3*a* and 3*c*). We eliminated the possibility that the antibodies to the extracellular domain of EGFR used for the immunoblot analysis shown in Figure 3*a* bind only to the unoccupied form of EGFR (as a result of competition with EGF, matuzumab or cetuximab) by performing the immunoblot analysis shown in Figures 3*b* and 3*c* with antibodies to the intracellular domain of EGFR. These results thus suggested that downregulation of EGFR is impaired in cells treated with matuzumab or cetuximab, likely explaining the failure of these antibodies to activate downstream signaling by Akt and Erk.

To confirm that the inability of the anti-EGFR mAbs to induce EGFR downregulation is attributable to a failure to induce internalization-dependent receptor degradation, we treated serum-deprived H292 cells with matuzumab or EGF for 4 hr and then examined the expression of EGFR by immunofluorescence analysis (Fig. 3*d*) or flow cytometry (Fig. 3*e*). Whereas EGFR was localized at the cell surface in control cells, treatment with EGF resulted in internalization and a decrease in the fluorescence intensity of EGFR. In contrast, EGFR remained at the surface of cells treated with matuzumab. These data suggested that, in contrast to EGF-EGFR complexes, antibody-EGFR complexes remain at the cell surface and do not undergo internalization and degradation.

TABLE I – CHARACTERISTICS OF NSCLC CELL LINES

Cell line	*EGFR* mutation	*EGFR* copy number
H292	Wild type	Polysomy
H460	Wild type	Monosomy
Ma-1	del E746-A750	Gene amplification

Effects of matuzumab and cetuximab on EGF-induced signaling and cell survival

We next determined whether matuzumab or cetuximab inhibits ligand-dependent EGFR signal transduction. To examine also whether the effects of these antibodies are dependent on *EGFR* status, we studied 3 human NSCLC cell lines: 2 cell lines (H292, H460) that possess wild-type *EGFR* alleles and 1 (Ma-1) with an *EGFR* mutation in exon 19 that results in deletion of the residues E746–A750. Our recent fluorescence in situ hybridization analysis[31] revealed that *EGFR* copy number is increased (polysomy) in H292 cells and that H460 cells exhibit monosomy for *EGFR*. Ma-1 cells were also found to manifest *EGFR* amplification (Table I).[31] We treated serum-deprived cells of the 3 NSCLC lines with

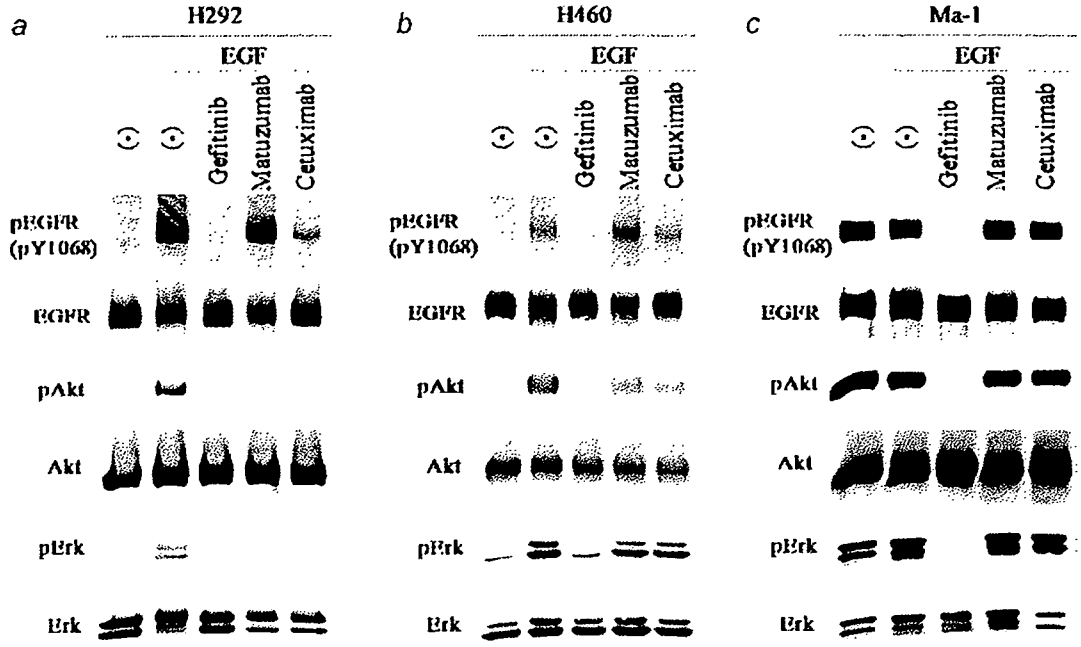

FIGURE 4 – Effects of matuzumab and cetuximab on EGF-induced EGFR signaling. H292 (*a*), H460 (*b*) and Ma-1 (*c*) cells were deprived of serum overnight and then incubated first for 15 min in the absence or presence of matuzumab (200 nM), cetuximab (100 nM) or gefitinib (10 μM) and then for an additional 15 min in the additional absence or presence of EGF (100 ng/ml). Cell lysates were subjected to immunoblot analysis with antibodies to phosphorylated forms of EGFR (pY1068), Akt or Erk as well as with those to total EGFR (the extracellular domain), Akt or Erk.

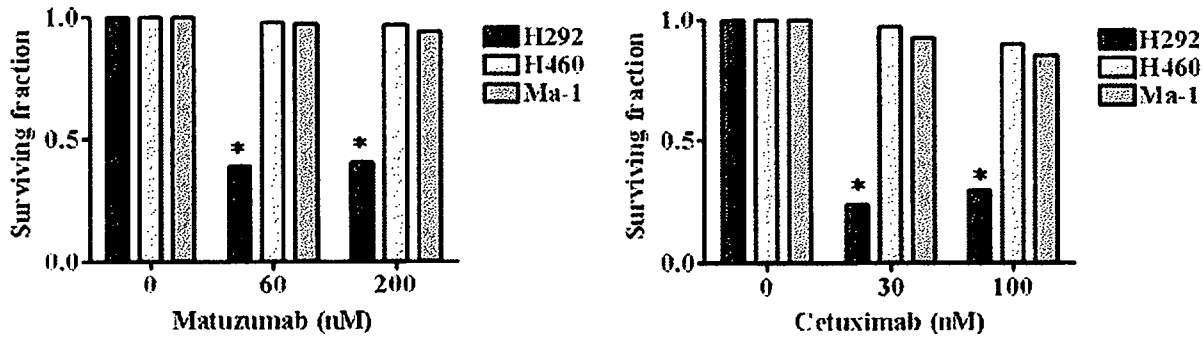

FIGURE 5 – Effects of matuzumab and cetuximab on cell survival. H292, H460 or Ma-1 cells were plated at a density of 200 cells per 25-cm^2 flask in triplicate and cultured for 7 days in the presence of the indicated concentrations of matuzumab or cetuximab. They were then incubated with medium alone for 7 days before determination of the number of colonies containing >50 cells for calculation of the surviving fraction. Data are means of triplicates from a representative experiment. *$p < 0.001$ *versus* the corresponding value for cells not exposed to mAb (Student's *t*-test).

matuzumab, cetuximab or gefitinib for 15 min and then stimulated them with EGF for 15 min. Gefitinib prevented the phosphorylation of EGFR, Akt, and Erk induced by EGF in H292 (Fig. 4*a*) and H460 (Fig. 4*b*) cells. The level of EGFR phosphorylation in EGF-treated H292 or H460 cells was not substantially affected by matuzumab or cetuximab, likely because these antibodies also induce EGFR phosphorylation. However, whereas matuzumab and cetuximab did not substantially affect EGF-dependent phosphorylation of Akt or Erk in H460 cells, they markedly inhibited these effects of EGF in H292 cells. As we showed previously,[31] EGFR, Akt, and Erk are constitutively activated in the *EGFR* mutant cell line Ma-1 cell (Fig. 4*c*). Furthermore, whereas gefitinib blocked the phosphorylation of each of these 3 proteins in Ma-1 cells, matuzumab and cetuximab did not.

Finally, we performed a clonogenic assay to determine whether cell survival is affected by the differences in EGF-dependent signaling among H292, H460 and Ma-1 cells after treatment with matuzumab or cetuximab (Fig. 5). Matuzumab and cetuximab each induced a marked reduction in the survival rate of H292 cells, consistent with the inhibition of EGF-dependent EGFR downstream signaling by these antibodies in these cells. In contrast, neither mAb affected the survival of H460 or Ma-1 cells, consistent with the lack of inhibition of EGF-dependent or constitutive EGFR downstream signaling by matuzumab or cetuximab in these cell lines. These results suggested that the effects of matuzumab and cetuximab on EGF-dependent or constitutive EGFR downstream signaling are correlated with their effects on cell survival in NSCLC cell lines.

Discussion

The effectiveness of treatment with anti-EGFR mAbs has been thought to be based on prevention of ligand binding to EGFR and consequent inhibition of EGFR activation.[18,25,26] Matuzumab and cetuximab have recently been developed as EGFR-inhibitory mAbs for clinical use.[17–22,25] A structural study revealed that cetuximab binds to the extracellular ligand binding domain (domain III) of EGFR,[25] and matuzumab is also thought to bind to domain III on the basis of its observed competition with EGFR ligands.[18] We have now shown that matuzumab and cetuximab induced phosphorylation of EGFR at several sites, including Y845, Y1068 and Y1173. These findings are consistent with previous observations that mAb 225, the mouse mAb equivalent to cetuximab, is able to induce EGFR dimerization and activation.[38,39] Cetuximab was also recently shown to induce phosphorylation of EGFR in head and neck squamous cell carcinoma cell lines[29] as well as in NSCLC cell lines including H292.[40] These in vitro results appear to contradict observations that matuzumab and cetuximab inhibit EGFR phosphorylation in vivo.[28,41,42] This apparent discrepancy may be due to the more complex cellular environment in vivo, including the presence of stromal cells that interact with tumor cells. We have also now shown that gefitinib, a specific EGFR-TKI, completely blocked EGFR phosphorylation induced by matuzumab or cetuximab, confirming that this effect of the antibodies is dependent on the intrinsic tyrosine kinase activity of EGFR. Furthermore, our cross-linking analysis showed that matuzumab as well as cetuximab activated EGFR through induction of receptor dimerization. Although recent structural analysis has revealed that cetuximab restricts the range of the extended conformation of EGFR that is required for ligand-induced receptor dimerization,[25] matuzumab and cetuximab likely induce EGFR dimerization in a manner dependent on their immunologically bivalent binding capacities, as was previously shown for mAb 225.[39] We found that neutralizing antibodies to EGFR did not activate EGFR, even though they also recognize the external domain of EGFR and compete with EGFR ligands for receptor binding.[43] The neutralizing antibodies did not induce EGFR dimerization, however, likely accounting for their inability to activate EGFR. This difference in the ability to induce EGFR dimerization between matuzumab and cetuximab on the one hand and the neutralizing antibodies on the other might be due to differences in the corresponding binding sites on EGFR.

To examine the mechanism by which matuzumab and cetuximab exert antitumor effects despite their induction of EGFR activation, we investigated the effects of antibody-induced EGFR activation on EGFR downstream signal transduction. We found that EGFR activation induced by matuzumab or cetuximab was not accompanied by activation of downstream signaling pathways mediated by Akt and Erk, both of which play an important role in regulation of cell proliferation and survival.[35,36] Moreover, we found that the antibody-EGFR complexes were not removed from the plasma membrane, in contrast to the rapid receptor turnover induced by EGF. In response to ligand binding, the ligand-EGFR complex is rapidly internalized and then either recycled back to the cell surface or proteolytically degraded.[44–46] The internalized EGFR interacts with various signaling proteins that are important for sustained activation of the major signaling pathways mediated by PI3K-Akt and Erk.[44,47] The activity of the PI3K-Akt and Erk pathways is thus greatly reduced in cells that are defective in internalization of ligand-EGFR complexes as a result of their expression of a mutant form of dynamin.[37] Furthermore, expression in glioblastoma cells of an EGFR chimeric protein that does not undergo internalization resulted both in a reduction in the extent of EGFR-dependent activation of Akt and Erk as well as in inhibition of tumor growth.[48] These observations thus suggest that inhibition of EGFR turnover by matuzumab or cetuximab is likely responsible for the failure of these mAbs to activate Akt and Erk.

We examined the effects of matuzumab and cetuximab on EGF-dependent EGFR signaling and on cell survival in 3 NSCLC cell lines of differing *EGFR* status. The inhibition of EGF-dependent activation of Akt and Erk by these antibodies appeared related to the inhibition of clonogenic cell survival in the 3 cell lines. With regard to NSCLC cell lines harboring wild-type *EGFR* alleles, matuzumab and cetuximab markedly inhibited EGF-dependent phosphorylation of Akt and Erk in H292 cells but not in H460 cells. Both antibodies inhibited cell survival in H292 cells but not in H460 cells. These results suggest that the antitumor effects of matuzumab and cetuximab depend on inhibition of EGFR downstream signaling such as that mediated by Akt and Erk rather than on inhibition of EGFR itself. Our present data are consistent with previous observations that cetuximab did not inhibit EGFR phosphorylation completely even in cells sensitive to this antibody.[27,30] It is possible that the difference in sensitivity to matuzumab and cetuximab between the 2 cell lines expressing wild-type EGFR in the present study is due to the difference in gene copy number, given that we found an increase in *EGFR* copy number in H292 cells compared with that in H460 cells.[31] A previous clinical study showed that *EGFR* copy number correlated with the response to cetuximab treatment in individuals with colorectal cancer.[49] *EGFR* copy number was not determined by fluorescence in situ hybridization in previous clinical studies of NSCLC patients treated with matuzumab or cetuximab.[19,22–24] Several clinical studies of the therapeutic efficacy of anti-EGFR antibodies in NSCLC patients are underway, and investigation of the potential of molecular markers including *EGFR* copy number to predict clinical response is warranted. Matuzumab and cetuximab failed to inhibit both activation of Akt and Erk and clonogenic cell survival in Ma-1 cells, which express a mutant form of EGFR that shows an increased sensitivity to EGFR-TKIs such as gefitinib and erlotinib.[9–16] We recently showed that cells expressing EGFR mutants exhibit constitutive, ligand-independent receptor dimerization and activation,[31] likely explaining the lack of effect of matuzumab or cetuximab on EGFR signaling or cell survival in such cells. However, previous studies showed that cetuximab exerted an antitumor effect in a cell line with an *EGFR* mutation, whereas several other cell lines with *EGFR* mutations were resistant to cetuximab.[27,30] Our results are consistent with clinical observations showing that the presence of an *EGFR* mutation is not a major determinant of a positive response to cetuximab in individuals with NSCLC or colorectal cancer.[22,50,51]

In conclusion, we have shown that EGFR turnover is impaired in cells treated with the anti-EGFR mAbs matuzumab or cetuximab, resulting in inhibition of EGFR downstream signaling. Although our study is limited by the small number of cell lines analyzed, our findings provide important insight into the mechanisms by which anti-EGFR mAbs exert their antitumor effects, and they suggest that it may be possible to predict the therapeutic efficacy of such mAbs by assessment of EGFR signal transduction.

Acknowledgements

The authors thank Ms. Erina Hatashita and Ms. Yuki Yamada for technical assistance.

References

1. Carpenter G. Receptors for epidermal growth factor and other polypeptide mitogens. Annu Rev Biochem 1987;56:881–914.
2. Klapper LN, Kirschbaum MH, Sela M, Yarden Y. Biochemical and clinical implications of the ErbB/HER signaling network of growth factor receptors. Adv Cancer Res 2000;77:25–79.
3. Di Marco E, Pierce JH, Fleming TP, Kraus MH, Molloy CJ, Aaronson SA, Di Fiore PP. Autocrine interaction between TGF α and the EGF-receptor: quantitative requirements for induction of the malignant phenotype. Oncogene 1989;4:831–8.
4. Gullick WJ. Prevalence of aberrant expression of the epidermal growth factor receptor in human cancers. Br Med Bull 1991;47:87–98.
5. Salomon DS, Brandt R, Ciardiello F, Normanno N. Epidermal growth factor-related peptides and their receptors in human malignancies. Crit Rev Oncol Hematol 1995;19:183–232.

6. Ettinger DS. Clinical implications of EGFR expression in the development and progression of solid tumors: focus on non-small cell lung cancer. Oncologist 2006;11:358–73.
7. Harari PM. Epidermal growth factor receptor inhibition strategies in oncology. Endocr Relat Cancer 2004;11:689–708.
8. Mendelsohn J, Baselga J. Epidermal growth factor receptor targeting in cancer. Semin Oncol 2006;33:369–85.
9. Lynch TJ, Bell DW, Sordella R, Gurubhagavatula S, Okimoto RA, Brannigan BW, Harris PL, Haserlat SM, Supko JG, Haluska FG, Louis DN, Christiani DC, et al. Activating mutations in the epidermal growth factor receptor underlying responsiveness of non-small-cell lung cancer to gefitinib. N Engl J Med 2004;350:2129–39.
10. Paez JG, Janne PA, Lee JC, Tracy S, Greulich H, Gabriel S, Herman P, Kaye FJ, Lindeman N, Boggon TJ, Naoki K, Sasaki H, et al. EGFR mutations in lung cancer: correlation with clinical response to gefitinib therapy. Science 2004;304:1497–500.
11. Pao W, Miller V, Zakowski M, Doherty J, Politi K, Sarkaria I, Singh B, Heelan R, Rusch V, Fulton L, Mardis E, Kupfer D, et al. EGF receptor gene mutations are common in lung cancers from "never smokers" and are associated with sensitivity of tumors to gefitinib and erlotinib. Proc Natl Acad Sci USA 2004;101:13306–11.
12. Mitsudomi T, Kosaka T, Endoh H, Horio Y, Hida T, Mori S, Hatooka S, Shinoda M, Takahashi T, Yatabe Y. Mutations of the epidermal growth factor receptor gene predict prolonged survival after gefitinib treatment in patients with non-small-cell lung cancer with postoperative recurrence. J Clin Oncol 2005;23:2513–20.
13. Takano T, Ohe Y, Sakamoto H, Tsuta K, Matsuno Y, Tateishi U, Yamamoto S, Nokihara H, Yamamoto N, Sekine I, Kunitoh H, Shibata T, et al. Epidermal growth factor receptor gene mutations and increased copy numbers predict gefitinib sensitivity in patients with recurrent non-small-cell lung cancer. J Clin Oncol 2005;23:6829–37.
14. Cappuzzo F, Hirsch FR, Rossi E, Bartolini S, Ceresoli GL, Bemis L, Haney J, Witta S, Danenberg K, Domenichini I, Ludovini V, Magrini E, et al. Epidermal growth factor receptor gene and protein and gefitinib sensitivity in non-small-cell lung cancer. J Natl Cancer Inst 2005;97:643–55.
15. Hirsch FR, Varella-Garcia M, McCoy J, West H, Xavier AC, Gumerlock P, Bunn PA, Jr, Franklin WA, Crowley J, Gandara DR. Increased epidermal growth factor receptor gene copy number detected by fluorescence in situ hybridization associates with increased sensitivity to gefitinib in patients with bronchioloalveolar carcinoma subtypes: a Southwest Oncology Group Study. J Clin Oncol 2005;23:6838–45.
16. Tsao MS, Sakurada A, Cutz JC, Zhu CQ, Kamel-Reid S, Squire J, Lorimer I, Zhang T, Liu N, Daneshmand M, Marrano P, da Cunha Santos G, et al. Erlotinib in lung cancer—molecular and clinical predictors of outcome. N Engl J Med 2005;353:133–44.
17. Cunningham D, Humblet Y, Siena S, Khayat D, Bleiberg H, Santoro A, Bets D, Mueser M, Harstrick A, Verslype C, Chau I, Van Cutsem E. Cetuximab monotherapy and cetuximab plus irinotecan in irinotecan-refractory metastatic colorectal cancer. N Engl J Med 2004;351:337–45.
18. Astsaturov I, Cohen RB, Harari PM. EGFR-targeting monoclonal antibodies in head and neck cancer. Curr Cancer Drug Targets 2006;6:691–710.
19. Kollmannsberger C, Schittenhelm M, Honecker F, Tillner J, Weber D, Oechsle K, Kanz L, Bokemeyer C. A phase I study of the humanized monoclonal anti-epidermal growth factor receptor (EGFR) antibody EMD 72000 (matuzumab) in combination with paclitaxel in patients with EGFR-positive advanced non-small-cell lung cancer (NSCLC). Ann Oncol 2006;17:1007–13.
20. Seiden MV, Burris HA, Matulonis U, Hall JB, Armstrong DK, Speyer J, Weber JD, Muggia F. A phase II trial of EMD72000 (matuzumab), a humanized anti-EGFR monoclonal antibody, in patients with platinum-resistant ovarian and primary peritoneal malignancies. Gynecol Oncol 2007;104:727–31.
21. Graeven U, Kremer B, Sudhoff T, Killing B, Rojo F, Weber D, Tillner J, Unal C, Schmiegel W. Phase I study of the humanised anti-EGFR monoclonal antibody matuzumab (EMD 72000) combined with gemcitabine in advanced pancreatic cancer. Br J Cancer 2006;94:1293–9.
22. Hanna N, Lilenbaum R, Ansari R, Lynch T, Govindan R, Janne PA, Bonomi P. Phase II trial of cetuximab in patients with previously treated non-small-cell lung cancer. J Clin Oncol 2006;24:5253–8.
23. Thienelt CD, Bunn PA, Jr, Hanna N, Rosenberg A, Needle MN, Long ME, Gustafson DL, Kelly K. Multicenter phase I/II study of cetuximab with paclitaxel and carboplatin in untreated patients with stage IV non-small-cell lung cancer. J Clin Oncol 2005;23:8786–93.
24. Robert F, Blumenschein G, Herbst RS, Fossella FV, Tseng J, Saleh MN, Needle M. Phase I/IIa study of cetuximab with gemcitabine plus carboplatin in patients with chemotherapy-naive advanced non-small-cell lung cancer. J Clin Oncol 2005;23:9089–96.
25. Li S, Schmitz KR, Jeffrey PD, Wiltzius JJ, Kussie P, Ferguson KM. Structural basis for inhibition of the epidermal growth factor receptor by cetuximab. Cancer Cell 2005;7:301–11.
26. Adams GP, Weiner LM. Monoclonal antibody therapy of cancer. Nat Biotechnol 2005;23:1147–57.
27. Mukohara T, Engelman JA, Hanna NH, Yeap BY, Kobayashi S, Lindeman N, Halmos B, Pearlberg J, Tsuchihashi Z, Cantley LC, Tenen DG, Johnson BE, et al. Differential effects of gefitinib and cetuximab on non-small-cell lung cancers bearing epidermal growth factor receptor mutations. J Natl Cancer Inst 2005;97:1185–94.
28. Perez-Torres M, Guix M, Gonzalez A, Arteaga CL. Epidermal growth factor receptor (EGFR) antibody down-regulates mutant receptors and inhibits tumors expressing EGFR mutations. J Biol Chem 2006;281:40183–92.
29. Mandic R, Rodgarkia-Dara CJ, Zhu L, Folz BJ, Bette M, Weihe E, Neubauer A, Werner JA. Treatment of HNSCC cell lines with the EGFR-specific inhibitor cetuximab (Erbitux) results in paradox phosphorylation of tyrosine 1173 in the receptor. FEBS Lett 2006;580:4793–800.
30. Amann J, Kalyankrishna S, Massion PP, Ohm JE, Girard L, Shigematsu H, Peyton M, Juroske D, Huang Y, Stuart Salmon J, Kim YH, Pollack JR, et al. Aberrant epidermal growth factor receptor signaling and enhanced sensitivity to EGFR inhibitors in lung cancer. Cancer Res 2005;65:226–35.
31. Okabe T, Okamoto I, Tamura K, Terashima M, Yoshida T, Satoh T, Takada M, Fukuoka M, Nakagawa K. Differential constitutive activation of the epidermal growth factor receptor (EGFR) in non-small cell lung cancer cells bearing EGFR gene mutation and amplification. Cancer Res 2007;67:2046–53.
32. Waterfield MD, Mayes EL, Stroobant P, Bennet PL, Young S, Goodfellow PN, Banting GS, Ozanne B. A monoclonal antibody to the human epidermal growth factor receptor. J Cell Biochem 1982;20:149–61.
33. Ogiso H, Ishitani R, Nureki O, Fukai S, Yamanaka M, Kim JH, Saito K, Sakamoto A, Inoue M, Shirouzu M, Yokoyama S. Crystal structure of the complex of human epidermal growth factor and receptor extracellular domains. Cell 2002;110:775–87.
34. Schlessinger J. Ligand-induced, receptor-mediated dimerization and activation of EGF receptor. Cell 2002;110:669–72.
35. Scaltriti M, Baselga J. The epidermal growth factor receptor pathway: a model for targeted therapy. Clin Cancer Res 2006;12:5268–72.
36. Normanno N, De Luca A, Bianco C, Strizzi L, Mancino M, Maiello MR, Carotenuto A, De Feo G, Caponigro F, Salomon DS. Epidermal growth factor receptor (EGFR) signaling in cancer. Gene 2006;366:2–16.
37. Vieira AV, Lamaze C, Schmid SL. Control of EGF receptor signaling by clathrin-mediated endocytosis. Science 1996;274:2086–9.
38. Fan Z, Mendelsohn J, Masui H, Kumar R. Regulation of epidermal growth factor receptor in NIH3T3/HER14 cells by antireceptor monoclonal antibodies. J Biol Chem 1993;268:21073–9.
39. Fan Z, Lu Y, Wu X, Mendelsohn J. Antibody-induced epidermal growth factor receptor dimerization mediates inhibition of autocrine proliferation of A431 squamous carcinoma cells. J Biol Chem 1994;269:27595–602.
40. Raben D, Helfrich B, Chan DC, Ciardiello F, Zhao L, Franklin W, Baron AE, Zeng C, Johnson TK, Bunn PA, Jr. The effects of cetuximab alone and in combination with radiation and/or chemotherapy in lung cancer. Clin Cancer Res 2005;11:795–805.
41. Vanhoefer U, Tewes M, Rojo F, Dirsch O, Schleucher N, Rosen O, Tillner J, Kovar A, Braun AH, Trarbach T, Seeber S, Harstrick A, et al. Phase I study of the humanized antiepidermal growth factor receptor monoclonal antibody EMD72000 in patients with advanced solid tumors that express the epidermal growth factor receptor. J Clin Oncol 2004;22:175–84.
42. Luo FR, Yang Z, Dong H, Camuso A, McGlinchey K, Fager K, Flefleh C, Kan D, Inigo I, Castaneda S, Wong TW, Kramer RA, et al. Prediction of active drug plasma concentrations achieved in cancer patients by pharmacodynamic biomarkers identified from the geo human colon carcinoma xenograft model. Clin Cancer Res 2005;11:5558–65.
43. Johnson GR, Kannan B, Shoyab M, Stromberg K. Amphiregulin induces tyrosine phosphorylation of the epidermal growth factor receptor and p185erbB2. Evidence that amphiregulin acts exclusively through the epidermal growth factor receptor at the surface of human epithelial cells. J Biol Chem 1993;268:2924–31.
44. Sorkin A, Von Zastrow M. Signal transduction and endocytosis: close encounters of many kinds. Nat Rev Mol Cell Biol 2002;3:600–14.
45. Sorkin A. Internalization of the epidermal growth factor receptor: role in signalling. Biochem Soc Trans 2001;29:480–4.

46. Wiley HS, Burke PM. Regulation of receptor tyrosine kinase signaling by endocytic trafficking. Traffic 2001;2:12–18.
47. Wang Y, Pennock S, Chen X, Wang Z. Endosomal signaling of epidermal growth factor receptor stimulates signal transduction pathways leading to cell survival. Mol Cell Biol 2002;22:7279–90.
48. Liu KJ, Chen CT, Hu WS, Hung YM, Hsu CY, Chuang BF, Juang SH. Expression of cytoplasmic-domain substituted epidermal growth factor receptor inhibits tumorigenicity of EGFR-overexpressed human glioblastoma multiforme. Int J Oncol 2004;24:581–90.
49. Moroni M, Veronese S, Benvenuti S, Marrapese G, Sartore-Bianchi A, Di Nicolantonio F, Gambacorta M, Siena S, Bardelli A. Gene copy number for epidermal growth factor receptor (EGFR) and clinical response to antiEGFR treatment in colorectal cancer: a cohort study. Lancet Oncol 2005;6:279–86.
50. Barber TD, Vogelstein B, Kinzler KW, Velculescu VE. Somatic mutations of EGFR in colorectal cancers and glioblastomas. N Engl J Med 2004;351:2883.
51. Tsuchihashi Z, Khambata-Ford S, Hanna N, Janne PA. Responsiveness to cetuximab without mutations in EGFR. N Engl J Med 2005;353:208–9.

INTERNAL MEDICINE

PICTURES IN CLINICAL MEDICINE

Metastatic Serous Adenocarcinoma Arising in the Adnexa Uteri and Forming Pleural Cysts on the Diaphragmatic Pleura

Kunimitsu Kawahara[1], Masashi Kobayashi[2], Shinji Sasada[2], Kaoru Matsui[2] and Teruo Iwasaki[3]

Key words: pleural cyst, serous adenocarcinoma, adnexa uteri, pleural metastasis

Figure 1. Left thoracoscopy showed a pleural cyst measuring 1.5cm in diameter (arrow) and adjacent daughter cysts (arrowheads) on the diaphragmatic pleura.

(DOI: 10.2169/internalmedicine.46.6211)

A 74-year-old woman consulted our hospital complaining of cough that had persisted for the previous 3 months. Chest computed tomographic (CT) scan showed bilateral pleural effusion without any pulmonary lesions. Pleural effusion cytology showed adenocarcinoma. Barium enema, gastroduodenoscopy and abdominal CT did not demonstrate any abnormal findings. Serum CEA, NSE and CYFRA21-1 were 26.8 (cutoff: 5) ng/ml, 43.7 (cutoff: 10) ng/ml and 67.5 (cutoff: 3.5) ng/ml, respectively. After removal of 1,500 ml of pleural effusion, left thoracoscopy showed a few eccentric pleural cysts on the diaphragmatic pleura (Fig. 1). No pleural nodule suggestive of malignancy was recognized. The content of the cyst was clearly serous fluid. Pathologic examination of the cyst showed a small focus of adenocarci-

[1] Department of Pathology, Osaka Prefectural Medical Center for Respiratory and Allergic Diseases, Habikino, [2] Department of Thoracic Malignancy, Osaka Prefectural Medical Center for Respiratory and Allergic Diseases, Habikino and [3] Department of Thoracic Surgery, Osaka Prefectural Medical Center for Respiratory and Allergic Diseases, Habikino

Received for publication August 28, 2006; Accepted for publication October 4, 2006

Correspondence to Dr. Kunimitsu Kawahara, kawahara@hbk.pref.osaka.jp

DOI: 10.2169/internalmedicine.46.6211

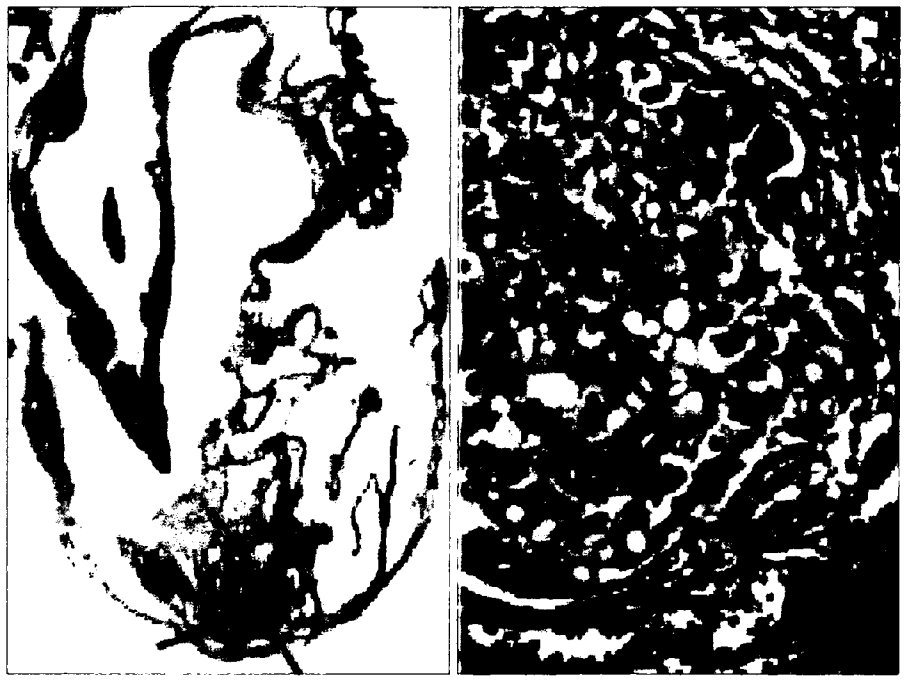

Figure 2. A: Microscopically, the pleural cyst was unilocular. A small focus of adenocarcinoma was recognized in the cyst wall (arrows). B: Most tumor cells had abundant clear or pale eosinophilic cytoplasm, oval nuclei and inconspicuous nucleoli. Stain: hematoxylin and eosin; magnification A: ×2.5, B: ×100.

noma (Fig. 2a, b). Immunohistochemical studies showed that these carcinoma cells were positive for AE1/AE3, EMA, CA125 and cytokeratin (CK)-7, but negative for CEA, TTF-1 and CK-20. The tentative diagnosis was Stage IV pulmonary adenocarcinoma. Systemic chemotherapy achieved stable disease. Six months later, the patient underwent surgery for right uterine adnexal tumor with diffuse peritoneal dissemination. Pathologic examination of the resected specimen demonstrated that the tumor was a poorly differentiated serous adenocarcinoma arising in the right adnexa uteri. Conclusively, we diagnosed pleural lesions as distant metastases of uterine adnexal serous adenocarcinoma. To our knowledge, the formation of these pleural cysts by metastatic carcinoma has not yet been reported in the literature. We propose two possible explanations for cyst formation by metastatic lesions: 1) localized edema in the submesothelial space due to carcinomatous obstruction of superficial vessels in the pleura caused pleural cysts; and 2) metastatic cancer cells in the pleura produced serous fluid in the submesothelial space and formed cystic lesions. The elucidation of its etiology, however, requires the accumulation of additional cases. Thoracic oncologists and pathologists should be aware of the varied gross manifestations of metastatic adenocarcinoma to the pleura and should bear in mind the differential diagnoses of pleural cysts.

© 2007 The Japanese Society of Internal Medicine
http://www.naika.or.jp/imindex.html

British Journal of Cancer (2008) 98, 907–914
© 2008 Cancer Research UK All rights reserved 0007–0920/08 $30.00
www.bjcancer.com

Multicentre prospective phase II trial of gefitinib for advanced non-small cell lung cancer with epidermal growth factor receptor mutations: results of the West Japan Thoracic Oncology Group trial (WJTOG0403)

K Tamura*[,1], I Okamoto[2], T Kashii[3], S Negoro[4], T Hirashima[5], S Kudoh[6], Y Ichinose[7], N Ebi[8], K Shibata[9], T Nishimura[10], N Katakami[11], T Sawa[12], E Shimizu[13], J Fukuoka[14], T Satoh[2] and M Fukuoka[15]

[1]Outpatients Treatment Center, National Cancer Center Hospital, 5-1-1, Tsukiji, Chuo-ku, Tokyo 104-0045, Japan; [2]Department of Medical Oncology, Kinki University School of Medicine, 377-2, Ohno-higashi, Sayama, Osaka 589-8511, Japan; [3]Department of Clinical Oncology, Osaka City General Hospital, 2-13-22, Miyakojima-hondori, Miyakojima, Osaka 534-0021, Japan; [4]Department of Thoracic Oncology, Hyogo Cancer Center, 13-70, Akashi, Kitaouji, Hyogo 673-8558, Japan; [5]Department of Thoracic Malignancy, Osaka Prefectural Medical Center for Respiratory and Allergic Diseases, 3-7-1, Habikino, Habikino, Osaka 583-8588, Japan; [6]Department of Respiratory Medicine, Osaka City University Medical School, 1-5-7, Asahi, Abeno, Osaka 545-8586, Japan; [7]Department of Thoracic Oncology, National Kyusyu Cancer Center, 3-1-1, Nodame, Minami, Fukuoka 811-1347, Japan; [8]Department of Respiratory Medicine, Iizuka Hospital, 3-83, Yoshio, Iizuka, Fukuoka 820-8505, Japan; [9]Department of Medicine, Koseiren Takaoka Hospital, 5-10, Eiraku, Takaoka, Toyama 933-8555, Japan; [10]Division of Respiratory Medicine, Kobe City General Hospital, 4-6, Minatojima-nakamachi, Chuo-ku, Kobe, Hyogo 650-0046, Japan; [11]Department of Integrated Oncology, Institute of Biomedical Research and Innovation, 2-2, Minatojima-minamimachi, Chuo-ku, Kobe, Hyogo 650-0047, Japan; [12]Department of Respiratory Medicine, Gifu Municipal Hospital, 7-1, Kashima, Gifu 500-8323, Japan; [13]Division of Medical Oncology and Respiratory Medicine, Faculty of Medicine, Tottori University, 36-1, Nishi-machi, Yonago, Tottori 683-8504, Japan; [14]Laboratory of Pathology, Toyama University Hospital, Toyama, 2630, Sugitani, Toyama 930-0194, Japan; [15]Department of Medical Oncology, Kinki University School of Medicine, Sakai Hospital, 2-7-1, Harayamadai, Minami-ku, Sakai, Osaka 590-0132, Japan

The purpose of this study was to evaluate the efficacy of gefitinib and the feasibility of screening for epidermal growth factor receptor (*EGFR*) mutations among select patients with advanced non-small cell lung cancer (NSCLC). Stage IIIB/IV NSCLC, chemotherapy-naive patients or patients with recurrences after up to two prior chemotherapy regimens were eligible. Direct sequencing using DNA from tumour specimens was performed by a central laboratory to detect *EGFR* mutations. Patients harbouring *EGFR* mutations received gefitinib. The primary study objective was response; the secondary objectives were toxicity, overall survival (OS), progression-free survival (PFS), 1-year survival (1Y-S) and the disease control rate (DCR). Between March 2005 and January 2006, 118 patients were recruited from 15 institutions and were screened for *EGFR* mutations, which were detected in 32 patients – 28 of whom were enrolled in the present study. The overall response rate was 75%, the DCR was 96% and the median PFS was 11.5 months. The median OS has not yet been reached, and the 1Y-S was 79%. Thus, gefitinib chemotherapy in patients with advanced NSCLC harbouring *EGFR* mutations was highly effective. This trial documents the feasibility of performing a multicentre phase II study using a central typing laboratory, demonstrating the benefit to patients of selecting gefitinib treatment based on their *EGFR* mutation status.
British Journal of Cancer (2008) **98,** 907–914. doi:10.1038/sj.bjc.6604249 www.bjcancer.com
Published online 19 February 2008
© 2008 Cancer Research UK

Keywords: epidermal growth factor receptor (*EGFR*) mutation; gefitinib; non-small cell lung cancer (NSCLC); multicentre prospective phase II; central laboratory

Gefitinib, a tyrosine kinase inhibitor (TKI), is an orally active small molecule that functions as a selective epidermal growth factor receptor (*EGFR*) inhibitor (Ranson *et al*, 2002). Two phase II trials (Fukuoka *et al*, 2003; Kris *et al*, 2003) for previously treated non-small cell lung cancer (NSCLC) (IDEAL-1 and -2, respectively) have documented favourable objective responses in 14–18% of patients. However, in a phase III trial (Thatcher *et al*, 2005), no survival benefit of gefitinib was observed when compared with best-supportive care (BSC) for previously treated NSCLC. In contrast, we have seen a significant survival benefit of erlotinib compared with BSC as a salvage therapy (BR21); erlotinib is also an *EGFR*-TKI and its chemical structure, which is based on quinazoline, is quite similar to that of gefitinib (Shepherd *et al*, 2005). Although we do not know whether differences between gefitinib and erlotinib were responsible for these different outcomes, appropriate patient selection to identify good responders is likely crucial for revealing the clinical benefits of the *EGFR*-TKI family.

*Correspondence: Dr K Tamura;
E-mail: ketamura@ncc.go.jp
Received 4 October 2007; revised 11 January 2008; accepted 15 January 2008; published online 19 February 2008

Patient subset analyses of these randomised phase III trials or retrospective trials (Kaneda *et al*, 2004; Miller *et al*, 2004) clearly show the existence of populations that are more likely to respond to gefitinib and erlotinib, including women, patients with adenocarcinoma (especially with bronchial alveolar carcinoma (BAC)), nonsmokers and Asian patients (compared with Caucasians). Somatic mutations in specific regions of exons 18, 19 and 21 of the ATP-binding domain of *EGFR* have recently been shown to have strong associations with sensitivity to gefitinib or erlotinib (Lynch *et al*, 2004; Paez *et al*, 2004; Pao *et al*, 2004). Consistent with these findings, the frequencies of these *EGFR* mutations were higher in women, patients with adenocarcinoma, nonsmokers and Asians, all of whom are among the more frequent responders, as mentioned above (Shigematsu *et al*, 2005). There are two characteristic types of *EGFR* mutations. One is the presence of in-frame deletions, including the amino acids at codons 746–750 in exon 19, and the other is an amino-acid substitution at codon 858 (L858R) in exon 21. Recent analyses (Bell *et al*, 2005) of phase II and III trials for *EGFR*-TKI, in which patients were not selected based on their mutation status, have suggested that *EGFR* mutations are correlated with response to therapy but are not correlated with overall survival (OS). Furthermore, *EGFR* gene amplification/copy number (Cappuzzo *et al*, 2005; Hirsch *et al*, 2005) or overexpression (Hirsch *et al*, 2003) has been shown to be a more useful prognostic marker of response to gefitinib treatment. Patient selection according to *EGFR* mutation status may yield a superior survival rate by excluding patients who are unlikely to respond to gefitinib treatment. However, other populations that might obtain a clinical benefit from gefitinib treatment, even in the absence of *EGFR* mutation, may exist.

Three Japanese groups (Asahina *et al*, 2006; Inoue *et al*, 2006; Yoshida *et al*, 2007) have reported prospective phase II studies of gefitinib for advanced-stage NSCLC that were designed to consider the *EGFR* mutation status of the patients. All of these studies have reported a high response rate and extended progression-free survival (PFS) period, compared with historical controls. However, all of these studies had a relatively short observation period, making the data preliminary. Moreover, the original sample size was calculated after patient selection, and a critical consideration of the suitability of the assay used to detect the mutations (which was performed using small paraffin-embedded specimens obtained from bronchoscopic biopsies), and the estimated *EGFR*-positive rate were lacking. Additionally, all the trials were conducted at single institutions located in one small area of Japan. Thus, the published data may not be representative of the situation found in general clinical practice throughout Japan and therefore may not directly translate to the general feasibility of gefitinib treatment in Japan.

In view of this situation, we performed a multicentre prospective phase II trial of gefitinib for advanced NSCLC harbouring *EGFR* mutations. We prospectively registered patients from 15 different institutes in Japan at the beginning of *EGFR* mutation screening using a central database. Whether or not tissue was available from a bronchoscopic biopsy or surgery was not an inclusion criterion. All the clinical samples from the registered patients were delivered to a central laboratory that then determined the *EGFR* mutation status or the histological BAC features. The analysis of the survival data was based on a minimum observation period of at least 15 months from the time of entry of the last patient.

MATERIALS AND METHODS

Eligibility criteria

Eligible patients had histologically confirmed stage III NSCLC for which thoracic irradiation was not indicated or were stage IV. Chemotherapy-naive patients or those who had previously received up to two prior chemotherapy regimens, including those performed in an adjuvant setting, were eligible. Other eligibility criteria included an age $\geqslant$20 years, measurable disease, the availability of sufficient amounts of tumour specimen for *EGFR* mutation analysis, an Eastern Cooperative Oncology Group performance status of 0–2, adequate organ function (WBC $\leqslant 3000\,\mu l^{-1}$, platelets $\geqslant 75\,000\,\mu l^{-1}$, AST and ALT $\leqslant 100\,IU\,l^{-1}$, serum creatinine $\leqslant$ twice the upper limit of the reference range; $P_{aO2} \geqslant 60$ mm Hg). The exclusion criteria included pulmonary fibrosis, the presence of symptomatic brain metastasis, active concomitant malignancy, severe heart disease, active gastrointestinal bleeding and continuous diarrhoea. All the patients signed a written informed consent form. Approval of this study and the gene analyses were obtained from the Institutional Review Board and the Ethics Committee of each hospital.

EGFR gene analysis

Tumour specimens were obtained using bronchial fiberscope or surgical procedures. The specimens were fixed with formalin and embedded in paraffin. Four slices (4–5 μm) from the embedded block were sent to a central laboratory (Mitsubishi Chemical Safety Institute Ltd., Ibaraki, Japan) for genetic analysis. Most of the tumour specimens were available prior to the registration of this study. Genomic DNA was isolated from specimens using QIAamp Micro kits (QIAGEN KK, Tokyo, Japan). The *EGFR* mutations in exons 18, 19 and 21, as previously reported (Lynch *et al*, 2004; Paez *et al*, 2004), were determined using polymerase chain reaction (PCR) amplification and intron–exon boundary primers according to the published method. An *EGFR* registrant mutation in exon 20, which was reported by Pao *et al* (2005) was also examined using PCR and the previously reported primers. Polymerase chain reaction was performed using a Gene Amp PCR System 9700 (Applied Biosystems, Foster City, CA, USA), and the PCR products were confirmed using a Bioanalyzer 2100 (Agilent Technologies Inc., Santa Clara, CA, USA), then sequenced directly using the Big Dye Terminator v3.1 Cycle Sequencing Kit (Applied Biosystems) and ABI PRISM 3100 (Applied Biosystems). All sequencing reactions were performed in both forward and reverse directions and were analysed using the Basic Local Alignment Search Tool (BLAST); all the electropherograms were reanalysed by visual inspection to check for mutations. The presence of an *EGFR* mutation was confirmed using at least three independent PCR.

All sequence data were sent from the central laboratory to Kinki University. A principle investigator then confirmed whether or not the *EGFR* mutation status was positive, and the results were sent to the West Japan Thoracic Oncology Group (WJTOG) data centre. The data centre then informed each participating centre of the results of the genetic analysis and requested that the eligibility criteria of the patients be rechecked to insure that only *EGFR*-positive subjects were registered in the trial. Each tumour was categorised according to histology by a pulmonary pathologist (JF). The percentage of area exhibiting a BAC pattern was also examined to determine the WHO pathological category.

Treatment plan

Gefitinib (250 mg day^{-1}) was administered once daily. Treatment was continued uninterrupted until disease progression or intolerable toxicity (grade 4 nonhaematological toxicities, any incidents of interstitial pneumonia or a treatment delay of more than 2 weeks because of adverse effects). Gefitinib administration was delayed if the patient's leukocyte and platelet counts were lower than 1500 and 5000 μl^{-1}, respectively, and was withheld until these counts had recovered. Gefitinib administration was also delayed if grade 3 or greater nonhaematological toxicities without nausea, vomiting or alopecia occurred and was withheld until recovery to grade 2.

© 2008 Cancer Research UK